

Optical conductivity in graphene: hydrodynamic regime

B.N. Narozhny^{1,2}

¹*Institut für Theorie der kondensierten Materie, Karlsruhe Institute of Technology, 76128 Karlsruhe, Germany*

²*National Research Nuclear University MEPhI (Moscow Engineering Physics Institute), 115409 Moscow, Russia*

(Dated: September 30, 2019)

A recent measurement of the optical conductivity in graphene [P. Gallagher *et.al*, *Science* **364**, 158 (2019)] offers a possibility of experimental determination of microscopic time scales describing scattering processes in the electronic fluid. In this paper, I report a theoretical calculation of the optical conductivity in graphene at arbitrary doping levels, within the whole “hydrodynamic” temperature range, and for arbitrary non-quantizing magnetic fields. The obtained results are in good agreement with the available experimental data.

Recent experiments^{1–8} indicate that charge carriers in graphene at nearly room temperatures may exhibit a hydrodynamic flow^{9,10}. Traditional linear-response transport measurements uncovered such remarkable features as the strong violation of the Wiedemann-Franz law³ and superballistic transport⁵. In this type of experiments all information about the flow of electrons is extracted from a small number of measured resistances^{2,4,5,8} and Johnson noise power³. Additional information about the flow can be obtained by current density imaging^{7,11,12} or terahertz spectroscopy¹. The latter experiment yields the optical conductivity which can be used to extract information about the electron-electron and electron-impurity scattering rates in graphene¹.

Hydrodynamic theory of electronic transport^{9,10} can be formulated similarly to the usual hydrodynamics¹³ with the important caveat: the total momentum of the electronic system in a solid is not, strictly speaking, a conserved quantity. In general, this means that one can only hope to observe electronic hydrodynamics in an intermediate temperature window where the electron-electron interaction is the dominant scattering mechanism in the problem⁹. In the specific case of graphene, there is an additional circumstance due to the linearity of the excitation spectrum: the momentum density is proportional to the energy current^{9,10,14–16} (rather than the “mass” current as in the usual hydrodynamics¹³). Hence it is the electrical (rather than the thermal) conductivity that appears in the hydrodynamic theory of electronic transport in graphene as a dissipative coefficient^{14–16}.

In traditional hydrodynamics, dissipative processes are described by three coefficients¹³: the shear and bulk viscosities and the thermal conductivity. In graphene, the bulk viscosity vanishes^{9,10,15}, leaving the shear viscosity as the only dissipative coefficient in the generalized Navier-Stokes equation^{14–16}. Under the assumption of approximate conservation of the particle number in each of the two bands in graphene¹⁷, electronic hydrodynamics describes two macroscopic quasiparticle currents (the electric and “imbalance” currents^{14–17}). Dissipative corrections to these currents due to electron-electron interaction are described by a 2×2 matrix of coefficients¹⁰. In addition, disorder scattering not only contributes to these coefficients, but also determines a correction to the

energy current¹⁵ yielding the thermal conductivity¹⁷. As a result, the electric and energy currents are relaxed by two different scattering mechanisms leading to the violation of the Wiedemann-Franz law³. The effect is especially pronounced at charge neutrality³ where the two currents are completely decoupled.

Assuming the applicability of the kinetic approach, one can derive the dissipative coefficients appearing in hydrodynamics starting with the Boltzmann equation and the local equilibrium distribution function^{9,10,14–16,18}. The resulting viscosities and conductivities are temperature- and material-dependent constants¹⁸. In contrast, calculations based on the Kubo formula yield frequency-dependent viscosities^{19–21} and conductivities^{19,22}. The frequency-dependent (optical) conductivity is experimentally measurable²² even in the hydrodynamic regime¹.

In this paper I extend the kinetic derivation of the dissipative corrections to the hydrodynamic quantities in graphene allowing for the low-frequency optical conductivity (in general, hydrodynamics is valid for frequencies which are much lower than the typical scattering rate associated with equilibration processes, $\omega\tau_{ee} \ll 1$). I also use the kinetic theory to extend the hydrodynamic-like macroscopic description²³ to higher frequencies where the results should be compared to those in the high-frequency collisionless regime^{21,24–29}.

Previously, optical conductivity in the hydrodynamic regime in graphene was addressed in Refs. 30–34. A large part of that research was focused on the two limiting cases, charge neutrality and the degenerate regime. In the absence of the magnetic field, the results for these two limits can be combined in an interpolation formula³⁴

$$\sigma(\omega; \mathbf{q}=0) = \frac{A_1}{-i\omega + \tau_{\text{dis}}^{-1}} + \frac{A_2}{-i\omega + \tau_{ee}^{-1} + \tau_{\text{dis}}^{-1}}, \quad (1)$$

where A_i are temperature- and density-dependent constants, τ_{dis} is the elastic mean free time, and τ_{ee} is the typical time scale associated with the electron-electron interaction. Here I report the results of a rigorous calculation of $\sigma(\omega)$ for arbitrary carrier densities, temperatures (within the hydrodynamic range), and classical (non-quantizing) magnetic fields beyond the limiting behavior of Eq. (1), as well as of the microscopic times scales determining $\sigma(\omega)$.

I. UNCONVENTIONAL HYDRODYNAMICS IN GRAPHENE

Unconventional hydrodynamics in graphene was derived in Refs. 14,15 on the basis of the kinetic theory. The need for the derivation was dictated by the lack of symmetry in the problem – the electronic system in graphene is neither Galilean, nor Lorentz invariant. The former follows from the linearity of the excitation spectrum, while the latter is related to the classical, three-dimensional nature of the Coulomb interaction in graphene.

As in any other solid, electrons in graphene may scatter on lattice vibrations (phonons) and imperfections (typically referred to as “disorder”) and hence loose momentum. In this case, one can speak of hydrodynamics only within a limited parameter regime (e.g., at intermediate temperatures) where the electron-electron interaction is the dominant scattering mechanism in the problem. This “hydrodynamic” regime can be defined by the inequality

$$\tau_{ee} \ll \tau_{\text{dis}}, \tau_{e\text{-ph}}, \tau_R, \text{ etc}, \quad (2)$$

where $\tau_{e\text{-ph}}$ is the typical scale describing the electron-phonon interaction, τ_R is the quasiparticle “recombination” time and “etc” stands for any other scattering-related time scale in the problem.

Assuming the applicability of the kinetic (Boltzmann) equation at least in some subset of the hydrodynamic region, hydrodynamic equations can be derived from the kinetic equation following the standard procedure¹⁸.

Conservation of charge and energy can be expressed in terms of the continuity equations¹⁴⁻¹⁶

$$\partial_t n + \nabla_{\mathbf{r}} \cdot \mathbf{j} = 0, \quad (3a)$$

$$\partial_t n_E + \nabla_{\mathbf{r}} \cdot \mathbf{j}_E = e \mathbf{E} \cdot \mathbf{j}. \quad (3b)$$

where n is the carrier density, \mathbf{j} is the current (differing from the charge density and electric current by a multiplicative factor of the electric charge, e), n_E and \mathbf{j}_E are the energy density and current, and \mathbf{E} is the electric field ($e \mathbf{E} \cdot \mathbf{j}$ describing Joule heat). The continuity equation (3a) is valid in any electronic system, while Eq. (3b) neglects possible energy losses due to coupling to collective excitations (e.g., phonons, plasmons, etc.).

The main equations of the hydrodynamic theory, the Euler and Navier-Stokes equations (for ideal and viscous fluids, respectively), are based on the continuity equation for momentum density reflecting momentum conservation. In solids, electronic momentum can be treated as a conserved quantity only approximately, in the sense of Eq. (2). Hence, the generalized Navier-Stokes equation in graphene¹⁵ contains a weak disorder scattering term,

$$\begin{aligned} W(\partial_t + \mathbf{u} \cdot \nabla) \mathbf{u} + v_g^2 \nabla P + \mathbf{u} \partial_t P + e(\mathbf{E} \cdot \mathbf{j}) \mathbf{u} = \quad (3c) \\ = v_g^2 \left[\eta \Delta \mathbf{u} - \eta_H \Delta \mathbf{u} \times \mathbf{e}_B + e n \mathbf{E} + \frac{e}{c} \mathbf{j} \times \mathbf{B} \right] - \frac{\mathbf{j}_E}{\tau_{\text{dis}}}, \end{aligned}$$

where v_g is the Fermi velocity in graphene, \mathbf{u} is the hydrodynamic velocity, \mathbf{B} is the magnetic field, c is the speed of light, and W and P are the enthalpy and pressure, which are related to the energy density in graphene by the “equation of state”^{14,15}

$$W = n_E + P = \frac{3n_E}{2+u^2/v_g^2}. \quad (3d)$$

The shear, η , and Hall, η_H , viscosities in graphene were discussed theoretically in Ref. 16 and experimentally in Refs. 2,8.

Due to kinematic suppression of interband scattering in graphene^{10,17}, one may consider conservation of the particle number in each band. This leads to another continuity equation

$$\partial_t n_I + \nabla_{\mathbf{r}} \cdot \mathbf{j}_I = -\frac{n_I - n_{I,0}}{\tau_R}, \quad (3e)$$

where $n_{I,0}$ is the equilibrium “imbalance” density. The “imbalance” density and current¹⁷ (as well as n and \mathbf{j}) are related to the densities and currents in each band as

$$n = n_+ - n_-, \quad n_I = n_+ + n_-, \quad (3f)$$

$$\mathbf{j} = \mathbf{j}_+ - \mathbf{j}_-, \quad \mathbf{j}_I = \mathbf{j}_+ + \mathbf{j}_-. \quad (3g)$$

Finally, the quasiparticle currents \mathbf{j} and \mathbf{j}_I are not related to any conserved quantity and hence acquire dissipative corrections (similarly to the energy current in the traditional hydrodynamics¹³). The energy current in graphene is proportional to the momentum density and hence cannot be relaxed by electron-electron interaction. However, it can be relaxed by weak disorder (leading to the strong violation of the Wiedemann-Franz law³). Combining the dissipative corrections to the three macroscopic currents in graphene, one defines the second set of dissipative coefficients¹⁵

$$\mathbf{j} = n \mathbf{u} + \delta \mathbf{j}, \quad \mathbf{j}_I = n_I \mathbf{u} + \delta \mathbf{j}_I, \quad \mathbf{j}_E = W \mathbf{u} + \delta \mathbf{j}_E, \quad (3h)$$

$$\begin{pmatrix} \delta \mathbf{j} \\ \delta \mathbf{j}_I \\ \delta \mathbf{j}_E/T \end{pmatrix} = \hat{\Sigma} \begin{pmatrix} \mathbf{F}_{\mathbf{u}} - T \nabla \frac{\mu}{T} \\ T \nabla \frac{\mu}{T} \\ 0 \end{pmatrix} + \hat{\Sigma}_H \begin{pmatrix} \mathbf{F}_{\mathbf{u}} - T \nabla \frac{\mu}{T} \\ T \nabla \frac{\mu}{T} \\ 0 \end{pmatrix} \times \mathbf{e}_B, \quad (3i)$$

where $\mathbf{F}_{\mathbf{u}} = e \mathbf{E} + \frac{e}{c} \mathbf{u} \times \mathbf{B}$, while μ and μ_I are the chemical potentials conjugate to n and n_I , respectively. They are related to the chemical potentials μ_{λ} as

$$\mu = (\mu_+ + \mu_-)/2, \quad \mu_I = (\mu_+ - \mu_-)/2. \quad (3j)$$

In this paper I disregard thermoelectric effects¹⁷ and set $\mu_{\pm} = \mu$ (or $\mu_I = 0$).

In addition to Eqs. (3) the complete hydrodynamic theory includes Maxwell’s equations taking into account electromagnetic fields induced by inhomogeneities of the charge density similarly to the Vlasov self-consistency¹⁸. In solids typical velocities are rather small, $v_g \ll c$, and hence the Maxwell’s equations are usually reduced to electrostatics. In gated structures^{2,5,6,8} the electrostatics is controlled by the gate^{35,36} further simplifying the relation between the charge density and electric field.

II. DISSIPATIVE COEFFICIENTS

The dissipative coefficients $\widehat{\Sigma}$ and $\widehat{\Sigma}_H$ are related to the electrical conductivity¹⁰ (and are the counterpart of the thermal conductivity in traditional hydrodynamics¹³). In the absence of the magnetic field the Hall term vanishes, $\widehat{\Sigma}_H(B=0) = 0$. The matrix $\widehat{\Sigma}(B=0)$ simplifies at the Dirac point, where it is block diagonal, such that the electric current decouples from the other two. Moreover, at $n = 0$ the “hydrodynamic” contribution to \mathbf{j} vanishes [see Eq. (3h)], leaving the dissipative correction $\delta\mathbf{j}$ as the total current. This correction remains finite even in the absence of disorder,

$$e\delta\mathbf{j}(\mu=0) = \sigma_Q \mathbf{E}, \quad \sigma_Q = \mathcal{A}e^2/\alpha_g^2, \quad \mathcal{A} \approx 0.12, \quad (4)$$

where σ_Q is known as the “quantum” or “intrinsic” conductivity of graphene^{10,14,15,30–33,37,38}. The quantity σ_Q is a constant that depends on temperature only through the logarithmic renormalization of the coupling constant α_g ³⁹. Away from the Dirac point, matrix elements of $\widehat{\Sigma}$ may exhibit more pronounced temperature and density dependence, but within the framework of Ref. 15 they remain independent of frequency.

A. Kinetic theory approach

Within the standard approach¹⁸, one derives the hydrodynamic theory from the kinetic equation

$$\mathcal{L}f = \text{St}[f], \quad \mathcal{L} = \partial_t + \mathbf{v} \cdot \nabla_{\mathbf{r}} + (e\mathbf{E} + \frac{e}{c}\mathbf{v} \times \mathbf{B}) \cdot \nabla_{\mathbf{k}}. \quad (5)$$

Under the assumption of local equilibrium, Eq. (5) can be solved approximately

$$f = f^{(0)} + \delta f, \quad (6)$$

where $f^{(0)}$ is the local equilibrium distribution function (nullifying the collision integral due to electron-electron interaction) and δf is the nonequilibrium correction. The latter can be found within linear response:

$$\mathcal{L}f^{(0)} = \text{St}[\delta f]. \quad (7)$$

Linearizing the collision integral, one proceeds with the solution of the resulting linear integral equation (which, however nontrivial, is much simpler than the original nonlinear integro-differential equation). Macroscopic description corresponding to local equilibrium is the ideal (Euler) hydrodynamics, while the nonequilibrium correction is responsible for dissipative terms.

The reason one is justified in neglecting $\mathcal{L}\delta f$ in Eq. (7) is the long wavelength nature of hydrodynamics – macroscopic quantities are assumed to be varying slowly over long distances such that their gradients are small. Hence, gradients of the correction, $\nabla\delta f$, represent the second-order smallness in the hydrodynamic expansion (formally, in the so-called Knudsen number^{13,18}). Similar argument can be applied to the electric field. Magnetic field

is typically not treated within linear response¹⁵ leading to the field-dependent viscosity and Hall viscosity^{8,16,40–42}. Treating the time derivative in the Liouville’s operator in the same manner leads to frequency-dependent dissipative coefficients. In other words, instead of Eq. (7) yielding constant, field-independent viscosity and conductivity, one should solve the equation

$$\mathcal{L}\Big|_{\mathbf{B}=0} f^{(0)} + \partial_t \delta f + \frac{e}{c} [\mathbf{v} \times \mathbf{B}] \cdot \nabla_{\mathbf{k}} f = \text{St}_{ee}[\delta f] + \text{St}_{\text{dis}}[f]. \quad (8)$$

In this paper, I solve Eq. (8) focusing on the frequency- and field-dependent “effective conductivities” $\widehat{\Sigma}(\omega)$ and $\widehat{\Sigma}_H(\omega)$. A similar analysis of the frequency-dependent viscosity⁴³ will be reported elsewhere.

B. Dissipative corrections to macroscopic currents in graphene

A comprehensive derivation of the dissipative hydrodynamics in graphene was reported in Ref. 15. In comparison to Eq. (8) that calculation disregarded the time derivative, $\partial_t \delta f$, yielding frequency-independent dissipative coefficients. On the other hand, the other terms in the (linear) equation (8) were evaluated in all the details. In this Section I outline that calculation in order to make the present paper self-contained focusing on the essential changes that are necessary to evaluate optical conductivity. Technical details can be found in Ref. 15.

The main idea of the calculation^{14,15} is to formulate macroscopic equations for the three currents (3i) integrating the kinetic equation and expressing the non-equilibrium correction to the distribution function, δf , in terms of the dissipative corrections to the currents. To the resulting “three-mode” approximation, δf is (in graphene, single-particle states can be labeled by the band index $\lambda = \pm$ and momentum \mathbf{k} ; in what follows, these indices are often omitted for brevity).

$$\delta f = f^{(0)} \left[1 - f^{(0)} \right] h, \quad h_{\lambda\mathbf{k}} = \frac{v_{\lambda\mathbf{k}}}{v_g} \sum_{i=1}^3 \phi_i \mathbf{h}^{(i)}, \quad (9a)$$

with the “three modes” (not exhibiting the collinear scattering singularity^{9,14,15,32}) described by

$$\phi_1 = 1, \quad \phi_2 = \lambda, \quad \phi_3 = \frac{\epsilon}{T},$$

where $\epsilon = \epsilon_{\lambda\mathbf{k}}$ is the excitation energy ($v_{\lambda\mathbf{k}} = \partial\epsilon_{\lambda\mathbf{k}}/\partial\mathbf{k}$) and the vectors $\mathbf{h}^{(i)}$ are related to the dissipative corrections (3i) to the macroscopic currents (3h) as^{14,15}

$$\begin{pmatrix} \delta\mathbf{j} \\ \delta\mathbf{j}_I \\ \delta\mathbf{j}_E/T \end{pmatrix} = \frac{v_g T}{2} \widehat{M}_h \begin{pmatrix} \mathbf{h}^{(1)} \\ \mathbf{h}^{(2)} \\ \mathbf{h}^{(3)} \end{pmatrix}. \quad (9b)$$

The matrix \widehat{M}_h is expressed in terms of equilibrium densities and compressibilities (see Appendix A for their ex-

PLICIT form) as

$$\widehat{M}_h = \frac{\partial n}{\partial \mu} \widehat{\mathbf{m}}_h, \quad \widehat{\mathbf{m}}_h = \begin{pmatrix} 1 & \frac{xT}{\mathcal{T}} & 2\tilde{n}\frac{T}{\mathcal{T}} \\ \frac{xT}{\mathcal{T}} & 1 & \left[x^2 + \frac{\pi^2}{3}\right]\frac{T}{\mathcal{T}} \\ 2\tilde{n}\frac{T}{\mathcal{T}} & \left[x^2 + \frac{\pi^2}{3}\right]\frac{T}{\mathcal{T}} & 6\tilde{n}_E\frac{T}{\mathcal{T}} \end{pmatrix}, \quad (9c)$$

where \tilde{n} and \tilde{n}_E are the dimensionless carrier and energy densities, respectively, $x = \mu/T$, and

$$\mathcal{T} = 2\pi v_g^2 \frac{\partial n}{\partial \mu} = 2T \ln \left[2 \cosh \frac{\mu}{2T} \right].$$

Multiplying Eq. (8) by the velocity, $\mathbf{v}_{\lambda\mathbf{k}}$, and integrating over all single-particle states ($N = 4$ is the degeneracy factor), one finds the macroscopic equation for the electric current

$$N \sum_{\lambda} \int \frac{d^2k}{(2\pi)^2} \mathbf{v}_{\lambda\mathbf{k}} \mathcal{L} f_{\lambda\mathbf{k}}^{(0)} = \mathcal{I}_1[f] - \frac{\partial \delta \mathbf{j}}{\partial t} - \omega_B \mathbf{e}_B \times \mathcal{K}[\delta f]. \quad (10a)$$

The integrated collision integral, $\mathcal{I}_1[f]$, comprises the electron-electron and disorder scattering terms

$$\mathcal{I}_1 = N \sum_{\lambda} \int \frac{d^2k}{(2\pi)^2} \mathbf{v}_{\lambda\mathbf{k}} (\text{St}_{ee}[\delta f] + \text{St}_{\text{dis}}[f]) \equiv \mathcal{I}_1^{ee} + \mathcal{I}_1^{\text{dis}}. \quad (10b)$$

I assume the latter to be weak [see Eq. (2)] such that the τ -approximation is sufficient [with the (model- and energy-dependent) scattering time, τ_{dis} , assumed to have the appropriate value determined by T and μ], such that

$$\mathcal{I}_1^{\text{dis}} = -\mathbf{j}/\tau_{\text{dis}}. \quad (10c)$$

The generalized cyclotron frequency,

$$\omega_B = eBv_g^2/(c\mathcal{T}), \quad (10d)$$

and the vector quantity \mathcal{K}

$$\mathcal{K}[\delta f] = \mathcal{T}N \sum_{\lambda} \int \frac{d^2k}{(2\pi)^2} \frac{\mathbf{k}}{k^2} \delta f_{\lambda\mathbf{k}}, \quad (10e)$$

appear after integrating the Lorentz term. Substituting Eqs. (9) into the integral (10e), one finds¹⁵

$$\mathcal{K}[\delta f] = \frac{v_g T}{2} \frac{\partial n}{\partial \mu} \left[\mathbf{h}^{(1)} \tanh \frac{x}{2} + \mathbf{h}^{(2)} + \mathbf{h}^{(3)} \frac{T}{\mathcal{T}} \right]. \quad (10f)$$

Since Eq. (10a) differs from that considered in Ref. 15 by the time derivative term in the right-hand side only, one can anticipate that the frequency-dependent dissipative coefficients can be elucidated from the results of Ref. 15 by adding the frequency to τ_{dis}^{-1}

$$\tau_{\text{dis}}^{-1} \rightarrow \tau_{\text{dis}}^{-1} + \partial/\partial t \rightarrow \tau_{\text{dis}}^{-1} - i\omega.$$

The integrated Liouville's operator, collision integral, and Lorentz term in Eq. (10a) were evaluated in Ref. 15. To the linear order in \mathbf{u} (within linear response in \mathbf{E})

$$N \sum_{\lambda} \int \frac{d^2k}{(2\pi)^2} \mathbf{v}_{\lambda\mathbf{k}} \mathcal{L} f_{\lambda\mathbf{k}}^{(0)} = n \frac{\partial \mathbf{u}}{\partial t} + \frac{v_g^2}{2} \nabla n - \frac{v_g^2}{2} e \mathbf{E} \frac{\partial n}{\partial \mu} - \frac{1}{2} v_g^2 \frac{e}{c} \frac{\partial n}{\partial \mu} \mathbf{u} \times \mathbf{B}. \quad (10g)$$

Expressing the time derivative in terms of gradients with the help of the Euler equation [i.e., Eq. (3c) without the viscous terms and magnetic field], one may express the integrated Liouville's operator in terms of the gradient of the electro-chemical potential (in the absence of temperature gradients)

$$N \sum_{\lambda} \int \frac{d^2k}{(2\pi)^2} \mathbf{v}_{\lambda\mathbf{k}} \mathcal{L} f_{\lambda\mathbf{k}}^{(0)} = v_g^2 \left(\frac{2n^2}{3n_E} - \frac{1}{2} \frac{\partial n}{\partial \mu} \right) \left(\mathbf{F}_u - T \nabla \frac{\mu}{T} \right) - \left(\frac{2nn_I}{3n_E} - \frac{1}{2} \frac{\partial n_I}{\partial \mu} \right) T \nabla \frac{\mu_I}{T}.$$

Similarly to Eq. (10) one finds the macroscopic equation for the imbalance current. This time the kinetic equation is multiplied by $\lambda \mathbf{v}_{\lambda\mathbf{k}}$ which upon integration yields

$$N \sum_{\lambda} \lambda \int \frac{d^2k}{(2\pi)^2} \mathbf{v}_{\lambda\mathbf{k}} \mathcal{L} f_{\lambda\mathbf{k}}^{(0)} = \mathcal{I}_2[f] - \frac{\partial \delta \mathbf{j}_I}{\partial t} - \omega_B \mathbf{e}_B \times \mathcal{K}_I[\delta f]. \quad (11a)$$

In the right-hand side of Eq. (11a), the integrated Lorentz term in Eq. (11a) contains the vector quantity

$$\mathcal{K}_I[\delta f] = \mathcal{T}N \sum_{\lambda} \lambda \int \frac{d^2k}{(2\pi)^2} \frac{\mathbf{k}}{k^2} \delta f_{\lambda\mathbf{k}} = \frac{v_g T}{2} \frac{\partial n}{\partial \mu} \left[\mathbf{h}^{(1)} + \mathbf{h}^{(2)} \tanh \frac{x}{2} + x \mathbf{h}^{(3)} \right], \quad (11b)$$

and $\mathcal{I}_2[f]$ denotes the integrated collision integral [defined similarly to Eq. (10b), but with the extra factor of λ]. The left-hand side of Eq. (11a) can be evaluated similarly to that in Eq. (10) such that¹⁵

$$N \sum_{\lambda} \lambda \int \frac{d^2k}{(2\pi)^2} \mathbf{v}_{\lambda\mathbf{k}} \mathcal{L} f_{\lambda\mathbf{k}}^{(0)} = v_g^2 \left(\frac{2nn_I}{3n_E} - \frac{1}{2} \frac{\partial n_I}{\partial \mu} \right) \left(\mathbf{F}_u - T \nabla \frac{\mu}{T} \right) - \left(\frac{2n_I^2}{3n_E} - \frac{1}{2} \frac{\partial n_I}{\partial \mu} \right) T \nabla \frac{\mu_I}{T}.$$

Finally, the energy current \mathbf{j}_E is proportional to the momentum density and hence the Liouville's operator acting on the local equilibrium distribution function yields zero. The integrated collision integral in the equation for the energy current vanishes due to momentum conservation. As a result, the macroscopic equation for the energy current contains only the Lorentz and disorder scattering terms

$$0 = -\frac{\delta \mathbf{j}_E}{\tau_{\text{dis}}} - \frac{\partial \delta \mathbf{j}_E}{\partial t} - \omega_B \frac{\mathcal{T}}{T} \mathbf{e}_B \times \delta \mathbf{j}. \quad (12)$$

Combining the three macroscopic currents into a vector, one can write all three macroscopic equations as a single equation in the matrix form¹⁵

$$\widehat{\mathbf{m}}_n \begin{pmatrix} \mathbf{F}_u - T \nabla \frac{\mu}{T} \\ T \nabla \frac{\mu_I}{T} \\ 0 \end{pmatrix} = \left[\frac{\alpha_g^2 T^2}{2\mathcal{T}^2} \widehat{\boldsymbol{\tau}} + \frac{\pi}{\mathcal{T}} \left(\frac{1}{\tau_{\text{dis}}} + \frac{\partial}{\partial t} \right) \widehat{\mathbf{m}}_h \right] \widehat{\mathbf{m}}_n^{-1} \begin{pmatrix} \delta \mathbf{j} \\ \delta \mathbf{j}_I \\ \delta \mathbf{j}_E/T \end{pmatrix} + \pi \frac{\omega_B}{\mathcal{T}} \widehat{\mathbf{m}}_K \widehat{\mathbf{m}}_h^{-1} \mathbf{e}_B \times \begin{pmatrix} \delta \mathbf{j} \\ \delta \mathbf{j}_I \\ \delta \mathbf{j}_E/T \end{pmatrix}, \quad (13a)$$

where the dimensionless matrix $\widehat{\mathbf{m}}_n$ describes the integrated Liouville's operators in the equations for the quasiparticle currents,

$$\begin{pmatrix} \frac{2n^2}{3n_E} - \frac{1}{2} \frac{\partial n}{\partial \mu} & -\frac{2nn_I}{3n_E} + \frac{1}{2} \frac{\partial n_I}{\partial \mu} & 0 \\ \frac{2nn_I}{3n_E} - \frac{1}{2} \frac{\partial n_I}{\partial \mu} & -\frac{2n_I^2}{3n_E} + \frac{1}{2} \frac{\partial n}{\partial \mu} & 0 \\ 0 & 0 & 0 \end{pmatrix} = -\frac{1}{2} \frac{\partial n}{\partial \mu} \widehat{\mathbf{m}}_n, \quad \widehat{\mathbf{m}}_n = \begin{pmatrix} 1 - \frac{2\tilde{n}^2}{3\tilde{n}_E} \frac{\mathcal{T}}{\mathcal{T}} & \frac{\tilde{n}}{3\tilde{n}_E} \left[x^2 + \frac{\pi^2}{3} \right] \frac{\mathcal{T}}{\mathcal{T}} - \frac{x\mathcal{T}}{\mathcal{T}} & 0 \\ \frac{x\mathcal{T}}{\mathcal{T}} - \frac{\tilde{n}}{3\tilde{n}_E} \left[x^2 + \frac{\pi^2}{3} \right] \frac{\mathcal{T}}{\mathcal{T}} & \frac{1}{6\tilde{n}_E} \left[x^2 + \frac{\pi^2}{3} \right]^2 \frac{\mathcal{T}}{\mathcal{T}} - 1 & 0 \\ 0 & 0 & 0 \end{pmatrix}, \quad (13b)$$

the dimensionless matrix $\widehat{\mathbf{m}}_K$ describes the integrated Lorentz terms,

$$\widehat{\mathbf{m}}_K = \begin{pmatrix} \tanh \frac{x}{2} & 1 & \frac{\mathcal{T}}{T} \\ \frac{1}{\mathcal{T}} & \tanh \frac{x}{2} & x \\ \frac{\mathcal{T}}{T} & x & 2\tilde{n} \end{pmatrix}, \quad (13c)$$

the integrated collision integral due to electron-electron interaction is expressed in terms of the ‘‘scattering rates’’¹⁵,

$$\begin{pmatrix} \mathcal{I}_1^{ee} \\ \mathcal{I}_2^{ee} \\ 0 \end{pmatrix} = -\frac{v_g T}{2} \frac{\partial n}{\partial \mu} \begin{pmatrix} \tau_{11}^{-1} & \tau_{12}^{-1} & 0 \\ \tau_{12}^{-1} & \tau_{22}^{-1} & 0 \\ 0 & 0 & 0 \end{pmatrix} \begin{pmatrix} \mathbf{h}^{(1)} \\ \mathbf{h}^{(2)} \\ \mathbf{h}^{(3)} \end{pmatrix}, \quad \begin{pmatrix} \tau_{11}^{-1} & \tau_{12}^{-1} & 0 \\ \tau_{12}^{-1} & \tau_{22}^{-1} & 0 \\ 0 & 0 & 0 \end{pmatrix} = \frac{\alpha_g^2 N T^2}{8\pi \mathcal{T}} \widehat{\boldsymbol{\tau}}, \quad (13d)$$

and finally τ_{dis}^{-1} describing disorder scattering enters the equation together with the time derivative (as explained above).

Solving the linear equations (13) by usual methods¹⁵, one finds for $\mu_I = 0$ and neglecting temperature gradients

$$\begin{pmatrix} \delta \mathbf{j} \\ \delta \mathbf{j}_I \\ \delta \mathbf{j}_E/T \end{pmatrix} = \widehat{\mathbf{m}}_h \left(1 + \widehat{\boldsymbol{\mathfrak{S}}}_{xx}^{-1} \widehat{\boldsymbol{\mathfrak{S}}}_{xy} \widehat{\boldsymbol{\mathfrak{S}}}_{xx}^{-1} \widehat{\boldsymbol{\mathfrak{S}}}_{xy} \right)^{-1} \widehat{\boldsymbol{\mathfrak{S}}}_{xx}^{-1} \widehat{\mathbf{m}}_n \begin{pmatrix} \mathbf{F}_u - \nabla \mu \\ 0 \\ 0 \end{pmatrix} \quad (14a)$$

$$- \widehat{\mathbf{m}}_h \left(1 + \widehat{\boldsymbol{\mathfrak{S}}}_{xx}^{-1} \widehat{\boldsymbol{\mathfrak{S}}}_{xy} \widehat{\boldsymbol{\mathfrak{S}}}_{xx}^{-1} \widehat{\boldsymbol{\mathfrak{S}}}_{xy} \right)^{-1} \widehat{\boldsymbol{\mathfrak{S}}}_{xx}^{-1} \widehat{\boldsymbol{\mathfrak{S}}}_{xy} \widehat{\boldsymbol{\mathfrak{S}}}_{xx}^{-1} \widehat{\mathbf{m}}_n \mathbf{e}_B \times \begin{pmatrix} \mathbf{F}_u - \nabla \mu \\ 0 \\ 0 \end{pmatrix},$$

where

$$\widehat{\boldsymbol{\mathfrak{S}}}_{xx} = \frac{\alpha_g^2 T^2}{2\mathcal{T}^2} \widehat{\boldsymbol{\tau}} + \frac{\pi}{\mathcal{T}} \left(\frac{1}{\tau_{\text{dis}}} - i\omega \right) \widehat{\mathbf{m}}_h, \quad \widehat{\boldsymbol{\mathfrak{S}}}_{xy} = \pi \frac{\omega_B}{\mathcal{T}} \widehat{\mathbf{m}}_K. \quad (14b)$$

Eq. (14) provides a closed expression for the dissipative corrections to the three macroscopic currents in the hydrodynamic picture of electronic transport in graphene. This result generalizes the earlier static solution¹⁵ providing the dissipative contribution to optical conductivity. While at charge neutrality the dissipative correction represents the total electric current, see Eq. (3i), away from the Dirac point one has to take into account the time-dependent solution of the hydrodynamic equations, the Navier-Stokes equation (3c) and continuity equations. Such solution can be obtained in a closed analytic form in the two limiting cases, either close to charge neutrality or in the degenerate regime. These two cases will be considered in detail in the remainder of this paper. In the most general case (e.g., for $\mu \sim T$) the hydrodynamic equations have to be solved numerically. Such analysis is beyond the scope of the present paper and will be discussed elsewhere.

III. OPTICAL CONDUCTIVITY IN ZERO MAGNETIC FIELD

Consider first graphene in the absence of magnetic field. Then the dissipative correction to the electric current is given by the first line in Eq. (14), which now simplifies to

$$\begin{pmatrix} \delta \mathbf{j} \\ \delta j_I \\ \delta \mathbf{j}_{E/T} \end{pmatrix} = \widehat{\mathbf{m}}_h \mathbf{S}_{xx}^{-1} \widehat{\mathbf{m}}_n \begin{pmatrix} e\mathbf{E} - \nabla\mu \\ 0 \\ 0 \end{pmatrix}. \quad (15a)$$

The corresponding contribution to conductivity can then be formally expressed as

$$\delta\sigma(\omega) = (1 \ 0 \ 0) \widehat{\mathbf{m}}_h \mathbf{S}_{xx}^{-1} \widehat{\mathbf{m}}_n \begin{pmatrix} 1 \\ 0 \\ 0 \end{pmatrix}. \quad (15b)$$

In addition to Eq. (15b), the full electrical conductivity in graphene comprises also the ‘‘hydrodynamic’’ contribution, see the first term in the electric current, Eq. (3h). In order to distinguish between the two, I will refer to Eq. (15b) as the ‘‘kinetic’’ contribution³⁴.

A. Hydrodynamic contribution to optical conductivity

The hydrodynamic contribution to the optical conductivity should be obtained by solving the Navier-Stokes equation (3c). Focusing on the homogeneous ($q = 0$) solution, I may write Eq. (3c) in the form $[\delta \mathbf{j}_E(\mathbf{B} = 0) = 0]$

$$W \partial_t \mathbf{u} + \mathbf{u} \partial_t P = v_g^2 e n \mathbf{E} - \frac{W \mathbf{u}}{\tau_{\text{dis}}}. \quad (16a)$$

Looking for homogeneous solutions of the continuity equations (3a) and (3b), I conclude that

$$\partial_t n = 0, \quad \partial_t n_E = 0, \quad (16b)$$

hence the time derivative of pressure in the Navier-Stokes equation vanishes as well ($P = n_E/2$). Then the equation takes the form

$$W \mathbf{u} (\tau_{\text{dis}}^{-1} - i\omega) = v_g^2 e n \mathbf{E}, \quad (16c)$$

with the solution

$$n \mathbf{u} = \frac{v_g^2 n^2}{W} \frac{e \mathbf{E}}{\tau_{\text{dis}}^{-1} - i\omega}. \quad (16d)$$

The resulting hydrodynamic contribution to the optical conductivity is given by³⁰

$$\sigma_h(\omega) = \frac{e^2 v_g^2 n^2}{W} \frac{1}{\tau_{\text{dis}}^{-1} - i\omega}. \quad (17)$$

1. Hydrodynamic contribution to conductivity in the degenerate regime

In the degenerate regime, $x \gg 1$, the enthalpy and carrier density can be expressed in terms of the chemical potential,

$$W = 3P = \frac{3n_E}{2} = \frac{\mu^3}{\pi v_g^2} \left(1 + \frac{\pi^2}{3x^2}\right), \quad (18a)$$

$$n = \frac{\mu^2}{\pi v_g^2} \left(1 + \frac{\pi^2}{3x^2}\right). \quad (18b)$$

Substituting these expressions into Eq. (17) and keeping the leading correction only, one finds

$$\sigma_h(\omega) = \frac{e^2 \mu}{\pi} \frac{1}{\tau_{\text{dis}}^{-1} - i\omega} \left(1 - \frac{\pi^2}{3x^2}\right). \quad (19)$$

In the limit $x \rightarrow \infty$ the result (19) represents the total optical conductivity, since the dissipative correction (15a) vanishes, see below.

2. Hydrodynamic contribution to conductivity near charge neutrality

At charge neutrality, $n = 0$, the electrical current (3i) is completely determined by the dissipative correction (15a). For nonzero, but small carrier density, $x \ll 1$, the carrier and energy densities can be expanded as

$$n = \frac{NT^2}{2\pi v_g^2} 2x \ln 2 + \mathcal{O}(x^3), \quad (20a)$$

$$n_E = \frac{NT^3}{2\pi v_g^2} [3\zeta(3) + 2x^2 \ln 2] + \mathcal{O}(x^4). \quad (20b)$$

This yields the following solution (to the leading order in $x \ll 1$) of the Navier-Stokes equation (16c)

$$n \mathbf{u} = \frac{16 \ln^2 2}{9\pi \zeta(3)} x^2 T \frac{e \mathbf{E}}{\tau_{\text{dis}}^{-1} - i\omega} + \mathcal{O}(x^4).$$

The resulting contribution to the optical conductivity is

$$\sigma_h(\omega) = \frac{e^2 T}{\pi} \frac{16 \ln^2 2}{9\zeta(3)} \frac{x^2}{\tau_{\text{dis}}^{-1} - i\omega} + \mathcal{O}(x^4). \quad (21)$$

The numerical coefficient in Eq. (21) is of order unity,

$$\frac{16 \ln^2 2}{9\zeta(3)} \approx 0.71.$$

Close to charge neutrality, the result (21) is subleading to the kinetic contribution to conductivity, which I discuss next.

B. Kinetic contribution to optical conductivity

Consider now the second contribution to conductivity, Eq. (15b), which stems from the dissipative correction to the electric current (15a). Since the general expression is not transparent enough, I now consider the limiting cases.

1. Optical conductivity at charge neutrality

At charge neutrality, $x = 0$, the matrices $\widehat{\mathbf{m}}_h$ and $\widehat{\mathbf{m}}_n$ simplify,

$$\widehat{\mathbf{m}}_h = \begin{pmatrix} 1 & 0 & 0 \\ 0 & 1 & \frac{\pi^2}{6 \ln 2} \\ 0 & \frac{\pi^2}{6 \ln 2} & \frac{9\zeta(3)}{2 \ln 2} \end{pmatrix}, \quad \widehat{\mathbf{m}}_n = \begin{pmatrix} 1 & 0 & 0 \\ 0 & -\delta & 0 \\ 0 & 0 & 0 \end{pmatrix}, \quad (22a)$$

where $\zeta(z)$ is the Riemann's zeta function and

$$\delta = 1 - \frac{\pi^4}{162\zeta(3) \ln 2} \approx 0.28.$$

The matrix of the scattering rates simplifies as well since $\tau_{12}^{-1}(\mu=0) = 0^{14,15}$. As a result, the matrix $\widehat{\mathbf{S}}_{xx}$ has the block-diagonal form

$$\widehat{\mathbf{S}}_{xx} = \frac{\pi}{2T \ln 2} \left[\begin{pmatrix} \tau_{11}^{-1} & 0 & 0 \\ 0 & \tau_{22}^{-1} & 0 \\ 0 & 0 & 0 \end{pmatrix} + \left(\frac{1}{\tau_{\text{dis}}} - i\omega \right) \widehat{\mathbf{m}}_h \right], \quad (22b)$$

where the electric current decouples from the other two. In the absence of temperature gradients the correction $\delta \mathbf{j}_I$ vanishes [also $\delta \mathbf{j}_E(\mathbf{B}=0) = 0$]. This can be seen from Eq. (15a) where the source term (i.e., the external electric field) is only present in the electric current sector. The conclusion about the energy current can be reached already from Eq. (12).

At zero frequency, the resulting electrical conductivity is given by Eq. (4):

$$e\delta \mathbf{j} = \frac{2 \ln 2}{\pi} e^2 T \left(\frac{1}{\tau_{11}} + \frac{1}{\tau_{\text{dis}}} \right)^{-1} \mathbf{E} \xrightarrow{\tau_{\text{dis}} \rightarrow \infty} \sigma_Q \mathbf{E}.$$

The coefficient \mathcal{A} in Eq. (4) can be found by evaluating the scattering rate numerically^{14,15,32,37,38}

$$\mathcal{A} = 2(\ln 2) \alpha_g^2 T \tau_{11} \approx 0.12. \quad (23)$$

The explicit expression for τ_{11} is given in Appendix B. Note, that the above value of \mathcal{A} was calculated with the unscreened Coulomb potential. At charge neutrality, this is a reasonable approximation for weak coupling (i.e., $\alpha_g \ll 1$). For larger values of α_g , which may be more experimentally relevant, screening leads to a quantitatively significant change in \mathcal{A} .

Keeping the nonzero frequency in Eq. (22b), I find the optical conductivity in graphene at charge neutrality^{1,34},

$$\sigma(\omega; \mu=0) = \frac{2 \ln 2}{\pi} \frac{e^2 T}{-i\omega + \tau_{\text{dis}}^{-1} + \tau_{11}^{-1}}, \quad (24)$$

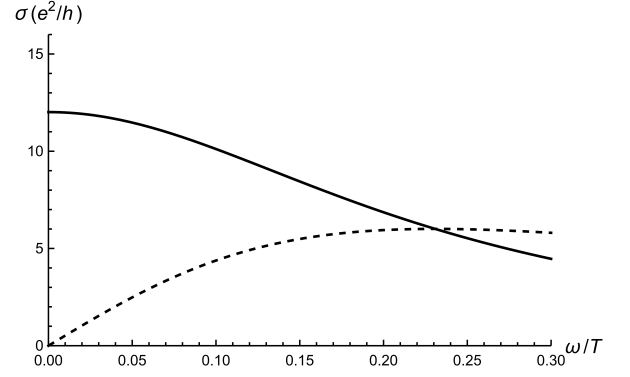


FIG. 1: Optical conductivity in graphene at charge neutrality. The real and imaginary parts of Eq. (24) are shown by the solid and dashed curves, respectively. The shown dependence appears to agree with the experimental data of Ref. 1 (see Fig. 3D of that reference). The curves were calculated with $\alpha_g = 0.23$ and $\tau_{\text{dis}}^{-1} = 0.8$ THz, the values taken from Ref. 1.

where τ_{11} is the same as in Eq. (23). This result is illustrated in Fig. 1.

2. Optical conductivity in the degenerate regime

Deep in the degenerate (or “Fermi-liquid”) regime, i.e. for $\mu \gg T$, the matrices in Eq. (15b) become degenerate. In particular, the matrix $\widehat{\mathbf{m}}_h$ determining the relation (9b) between the dissipative corrections to macroscopic currents and the nonequilibrium distribution function takes the form (up to exponentially small corrections)

$$\widehat{\mathbf{m}}_h = \begin{pmatrix} 1 & 1 & x \left[1 + \frac{\pi^2}{3x^2} \right] \\ 1 & 1 & x \left[1 + \frac{\pi^2}{3x^2} \right] \\ x \left[1 + \frac{\pi^2}{3x^2} \right] & x \left[1 + \frac{\pi^2}{3x^2} \right] & x^2 \left[1 + \frac{\pi^2}{x^2} \right] \end{pmatrix}, \quad (25)$$

where I have used the asymptotic expressions

$$\tilde{n} \approx \tilde{n}_I = \frac{x^2 + \pi^2}{2} + \frac{\pi^2}{6}, \quad \tilde{n}_E \approx \frac{x^3 + \pi^2 x}{6} + \frac{\pi^2 x}{6}, \quad \frac{\mathcal{T}}{T} \approx x.$$

The first of these equalities follows from the fact that in the degenerate regime only one band of carriers contributes to transport (the contribution of the other is exponentially suppressed; this is the reason why the two first rows in $\widehat{\mathbf{m}}_h$ are identical). In the limit $x \rightarrow \infty$ the factor $\pi^2/x^2 \rightarrow 0$ can be neglected. Then the third row of the matrix $\widehat{\mathbf{m}}_h$ is proportional to the first two, such that all three dissipative corrections in Eq. (9b) are proportional to each other. Now, regardless of the value of x , $\delta \mathbf{j}_E(\mathbf{B}=0) = 0$, see Eq. (12), and hence we conclude

$$\delta \mathbf{j}(x \rightarrow \infty) = \delta \mathbf{j}_I(x \rightarrow \infty) \approx \delta \mathbf{j}_E = 0. \quad (26a)$$

Note, that this result cannot be obtained from Eq. (15b) with the asymptotic form of $\widehat{\mathbf{m}}_h$ and other matrices since

in this limit the matrix \mathbf{S}_{xx} is degenerate (with or without the power law corrections). To find corrections to Eq. (26a) one has to either to keep track of exponentially small corrections to Eq. (25) or, alternatively, disregard the imbalance mode (since $\delta\mathbf{j} = \delta\mathbf{j}_I$ with exponential accuracy). Inverting the remaining 2×2 matrix, one finds

$$\delta\sigma(\omega) = \frac{\pi^3 e^2 \mu}{3x^2 [3x^2 \tau_{11}^{-1} + \pi^2 (\tau_{\text{dis}}^{-1} - i\omega)]}. \quad (26b)$$

The scattering rate τ_{11}^{-1} in the degenerate regime has the asymptotic form (neglecting screening; see Appendix C)

$$\tau_{11}^{-1}(x \gg 1) \approx \frac{4\pi}{3} \alpha_g^2 \frac{T^2}{\mu} = \frac{4\pi}{3} \alpha_g^2 \frac{\mu}{x^2}. \quad (26c)$$

Combining both contributions, Eqs. (26b) and (19), I find the optical conductivity in graphene as

$$\sigma(\omega) = \frac{e^2 \mu}{\pi} \frac{1}{\tau_{\text{dis}}^{-1} - i\omega} \left[1 - \frac{\tau_{11}^{-1}}{(3x^2/\pi^2)\tau_{11}^{-1} + \tau_{\text{dis}}^{-1} - i\omega} \right], \quad (27)$$

where the leading contribution is determined by disorder scattering only. The kinetic contribution to conductivity, $\delta\sigma$, is suppressed as x^{-2} . Moreover, the frequency dependence in $\delta\sigma$ becomes important only when it is comparable to $(3x^2/\pi^2)\tau_{11}^{-1} \gg \tau_{11}^{-1}$, see below.

3. Optical conductivity close to the Dirac point

Close to charge neutrality, i.e. for nonzero, but small carrier densities, $x \ll 1$, one finds corrections to Eq. (24). Expanding the matrices $\widehat{\mathbf{m}}_{h(n)}$ around the Dirac point, one finds

$$\widehat{\mathbf{m}}_{h(n)} = \widehat{\mathbf{m}}_{h(n)}(x=0) + \delta\widehat{\mathbf{m}}_{h(n)} + \mathcal{O}(x^3),$$

where $\widehat{\mathbf{m}}_{h(n)}(0)$ are given in Eq. (22a), while the leading-order corrections are given by

$$\delta\widehat{\mathbf{m}}_h = x \begin{pmatrix} 0 & \frac{1}{2\ln 2} & 2 \\ \frac{1}{2\ln 2} & 0 & \frac{x}{2\ln 2} \left[1 - \frac{\pi^2}{24\ln 2} \right] \\ 2 & \frac{x}{2\ln 2} \left[1 - \frac{\pi^2}{24\ln 2} \right] & 3x \left[1 - \frac{3\zeta(3)}{16\ln^2 2} \right] \end{pmatrix},$$

and

$$\delta\widehat{\mathbf{m}}_n = x$$

$$\times \begin{pmatrix} -\frac{8\ln 2}{27\zeta(3)} x & \frac{4\pi^2 \ln 2 - 27\zeta(3)}{2\ln 2} & 0 \\ -\frac{4\pi^2 \ln 2 - 27\zeta(3)}{2\ln 2} & \frac{\pi^2 x}{27\zeta(3) \ln 2} \left[1 - \frac{\pi^2}{48\ln 2} - \frac{\pi^2 \ln 2}{9\zeta(3)} \right] & 0 \\ 0 & 0 & 0 \end{pmatrix}.$$

The matrix \mathbf{S}_{xx} can be expanded in the same way, using the expansion of the scattering rates given in Appendix D. To the leading order, one finds

$$\mathbf{S}_{xx} = \mathbf{S}_{xx}(x=0) + \delta\mathbf{S}_{xx} + \mathcal{O}(x^3),$$

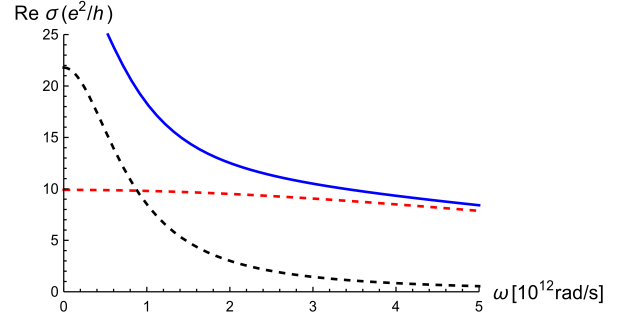


FIG. 2: Optical conductivity in weakly doped graphene at $n = 0.08 \text{ cm}^{-12}$ (or $E_F = 33 \text{ meV}$, the value used in Ref. 1, cf. Fig. 4B of that reference). The almost flat red dashed curve shows the real part of the kinetic contribution (15b), while the black dashed curve shows the real part of the hydrodynamic contribution (21). The real part of the full electrical conductivity (i.e., the sum $\delta\sigma + \sigma_h$) is shown by the solid blue curve. The curves were calculated with $\alpha_g = 0.23$, $T = 298 \text{ K}$, and $\tau_{\text{dis}}^{-1} = 0.8 \text{ THz}$, the values taken from Ref. 1.

where $\mathbf{S}_{xx}(x=0)$ is given by Eq. (22b) and

$$\delta\mathbf{S}_{xx} = \frac{\alpha_g^2}{8\ln^2 2} \delta\widehat{\mathbf{T}} + \frac{\pi}{2T \ln 2} (\tau_{\text{dis}}^{-1} - i\omega) \delta\widehat{\mathbf{m}}_h,$$

with

$$\delta\widehat{\mathbf{T}} = x \begin{pmatrix} \frac{x}{t_{11}^{(2)}} - \frac{1}{8\ln 2} \frac{x}{t_{11}^{(0)}} & 1/t_{12}^{(1)} & 0 \\ 1/t_{12}^{(1)} & \frac{x}{t_{22}^{(2)}} - \frac{1}{8\ln 2} \frac{x}{t_{22}^{(0)}} & 0 \\ 0 & 0 & 0 \end{pmatrix},$$

see Eqs. (D2) for notations.

Substituting the above expansions into Eq. (15b), one finds (see Appendix E for details)

$$\delta\sigma(\omega) = \sigma(\omega; \mu=0) + x^2 \delta\sigma^{(2)}(\omega) + \mathcal{O}(x^3), \quad (28a)$$

$$\begin{aligned} \delta\sigma^{(2)} = & \frac{\gamma_{11} e^2 T}{-i\omega + \tau_{\text{dis}}^{-1} + \tau_{11}^{-1}(0)} + \frac{\gamma_{12} e^2 T}{-i\omega + \tau_{\text{dis}}^{-1} + \gamma_{13} \tau_{22}^{-1}(0)} \\ & + \frac{e^2 T \left[\gamma_{31} \tau_{22}^{-1}(0) + \tilde{\gamma}_{32} (-i\omega + \tau_{\text{dis}}^{-1}) - \tilde{\gamma}_{33} / \tau_{12}^{(1)} \right]}{[-i\omega + \tau_{\text{dis}}^{-1} + \tau_{11}^{-1}(0)] [-i\omega + \tau_{\text{dis}}^{-1} + \gamma_{13} \tau_{22}^{-1}(0)]} \\ & + \frac{e^2 T \left[1/\tau_{11}^{(2)} - 1/[8\tau_{11}(0) \ln 2] \right]}{2\pi^2 [-i\omega + \tau_{\text{dis}}^{-1} + \tau_{11}^{-1}(0)]^2}, \end{aligned} \quad (28b)$$

where

$$\gamma_{11} \approx 0.075, \quad \gamma_{12} \approx 0.66, \quad \gamma_{13} \approx 3.59, \quad (28c)$$

$$\gamma_{31} \approx 0.81, \quad (28d)$$

$$\tilde{\gamma}_{32} = \gamma_{32} + \gamma_{41} \approx 0.91, \quad \tilde{\gamma}_{33} = \gamma_{42} - \gamma_{33} \approx 0.102. \quad (28e)$$

The total optical conductivity in the vicinity of the Dirac point is given by the sum of the leading term (24), the hydrodynamic contribution (21), and the above correction (28b). The two terms are compared in Fig. 2.

C. Comparison with the existing literature

Optical conductivity in graphene was already studied in several publications, so it is worthwhile to compare the above calculations to the previously known results.

The authors of the pioneering paper, Ref. 30, used general hydrodynamic arguments to find the optical conductivity at a generic charge density in the form

$$\sigma_{xx} = \sigma_Q + \sigma_h(\omega),$$

where σ_Q is the dissipative constant (4) and the hydrodynamic contribution is given (up to the choice of normalization) by Eq. (17). The specific value of σ_Q for graphene was calculated in Refs. 31,32,37,38.

Conductivity at the Dirac point in the absence of disorder was studied in detail in Ref. 32. The result of this paper is the same as Eq. (24) without the disorder scattering rate. The electron-electron scattering rate estimated in Ref. 32

$$\tau_{11}^{-1} \rightarrow \kappa \alpha_g^2 T, \quad \kappa = 3.646,$$

perfectly agrees with Eq. (D2a), where the numerical prefactor is $\kappa = 3.8$. Note that this value was obtained for unscreened Coulomb interaction.

Optical conductivity beyond charge neutrality was reported in Ref. 31. Here the authors combined the result of Ref. 32 with the hydrodynamic contribution previously reported in Ref. 30. In addition, the effect of disorder scattering was studied not only in the limit of weak disorder, but also for strong disorder, where the hydrodynamic approach is no longer valid. For weak disorder, the authors of Ref. 31 reported an expansion in the disorder strength.

The effect of disorder was also studied in Ref. 38 at charge neutrality. The reported zero-frequency conductivity agrees with Eq. (24) for weak disorder, $T\tau_{\text{dis}} \gg 1$. For stronger disorder, the authors of Ref. 38 took into account the effect of disorder scattering on the excitation spectrum in graphene which is beyond the scope of the present paper.

More recently, the interpolation formula (1) was suggested in Ref. 34 (see also Ref. 44) with the coefficient A_1 coinciding with that in Eq. (17) and the coefficient A_2 given by

$$A_2 \rightarrow e^2 \left[\frac{\mathcal{T}}{\pi} - \frac{v_g^2 n^2}{W} \right],$$

interpolating between the two limits: Eq. (24) at charge neutrality and Eq. (19) in the degenerate regime. In the former case, $n = 0$ (with $A_1 = 0$) and $\mathcal{T} = 2T \ln 2$, while in the latter case, $\mathcal{T} = \pi v_g^2 n^2 / W = \mu$, with $A_2 = 0$.

The interpolation formula Eq. (1) was used to interpret the result of recent measurements of the optical conductivity in graphene reported in Ref. 1. At charge neutrality, the experimental data appears to confirm the result

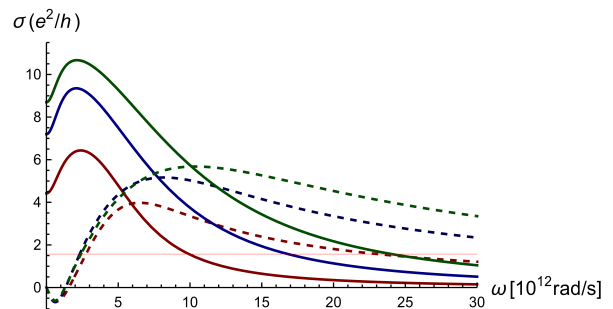


FIG. 3: Optical conductivity in graphene at charge neutrality in weak magnetic field, $B=0.1$ T. The real and imaginary parts of Eq. (31) are shown by the solid and dashed curves, with red, blue, and green (in ascending order for solid curves) corresponding to $T = 100, 200, 300$ K, respectively. The curves were calculated using the parameter values described in the main text based on the data of Ref. 1. The horizontal red line shows the universal conductivity Eq. (32) of free electrons in graphene in the high-frequency collisionless regime^{21,24–29} (actually observed at much higher frequencies).

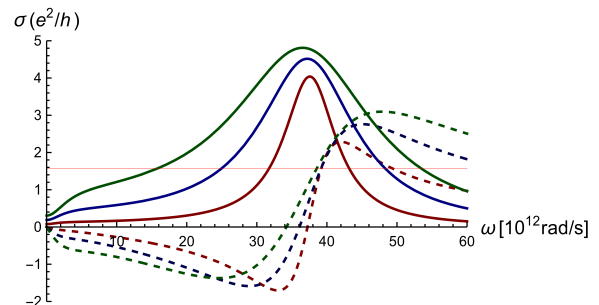


FIG. 4: Optical conductivity in graphene at charge neutrality at $B=1$ T. The real and imaginary parts of Eq. (31) are shown by the solid and dashed curves, with red, blue, and green (in ascending order for solid curves) corresponding to $T = 100, 200, 300$ K, respectively. The curves were calculated using the same parameter values as in Fig.3. The horizontal red line shows the universal conductivity Eq. (32) of free electrons in graphene in the high-frequency collisionless regime^{21,24–29} (actually observed at much higher frequencies).

Eq. (24) with $\tau_{\text{dis}} \gg \tau_{11}$, see Fig. 1, providing a reasonable (in line with previous measurements^{45,46}) estimate for α_g in real graphene. Data away from charge neutrality were measured at rather low charge densities, where the scattering rates Eq. (B5) exhibit only small deviations from their values at $\mu = 0$ (in agreement with the results of Ref. 1). Now, the kinetic contribution to optical conductivity Eq. (15b) has a Lorentzian-like shape as a function of ω [see Eqs. (14), (24), (26b), and (28)]. Hence, Eq. (15b) can be approximated by the second term in Eq. (1) by choosing the appropriate (phenomenological) values for τ_{ee} and τ_{dis} (as was done in Ref. 1, where the data was fitted by Eq. (1) with the electronic temperature and τ_{dis} used as fitting parameters). Note, that this procedure neglects renormalization of v_g due to electron-electron interaction^{10,32,39}.

IV. MAGNETOCONDUCTIVITY IN GRAPHENE

Consider now the effect of classical magnetic fields on the optical conductivity in graphene. The classical approach is justified at high enough temperatures where quantized transport is smeared out.

The general expression for the dissipative corrections to macroscopic currents is given by Eqs. (14). In the presence of the magnetic field, these corrections become “entangled” with the hydrodynamic velocity due to the Lorentz contribution to \mathbf{F}_u .

A. Magnetoconductivity at charge neutrality

The dissipative correction to the energy current was defined through Eq. (12). Substituting this relation into the Navier-Stokes equation (3c) at charge neutrality, one finds a stationary and uniform solution, $\mathbf{u} = 0$. Evaluating all matrices in Eqs. (14), one has to consider not only Eqs. (22), but also the matrix (13c). At $x=0$ I find

$$\widehat{\mathbf{m}}_K = \begin{pmatrix} 0 & 1 & 2 \ln 2 \\ 1 & 0 & 0 \\ 2 \ln 2 & 0 & 0 \end{pmatrix}. \quad (29)$$

Instead of multiplying the matrices in the general solution (14a), it appears to be more instructive to write Eq. (13a) explicitly at $x=0$ and proceed with solving the resulting equations.

Using Eq. (22a), the left-hand side of Eq. (13a) takes the form

$$\widehat{\mathbf{m}}_n \begin{pmatrix} e\mathbf{E} \\ 0 \\ 0 \end{pmatrix} = \begin{pmatrix} e\mathbf{E} \\ 0 \\ 0 \end{pmatrix}.$$

The longitudinal part of the right-hand side of Eq. (13a) is given by multiplying Eq. (22b) by $\widehat{\mathbf{m}}_h^{-1}$, see Eq. (22a),

$$\frac{\pi}{2T \ln 2} \left[\begin{pmatrix} \tau_{11}^{-1} & 0 & 0 \\ 0 & \tau_{22}^{-1} \delta^{-1} & -\tau_{22}^{-1} \frac{\pi^2}{27\zeta(3)\delta} \\ 0 & 0 & 0 \end{pmatrix} + \frac{1}{\tau_{\text{dis}}} - i\omega \right],$$

$$\sigma_{xx}(\omega) = \frac{2 \ln 2}{\pi} \frac{e^2 T (\tau_{\text{dis}}^{-1} - i\omega) (\delta^{-1} \tau_{22}^{-1} + \tau_{\text{dis}}^{-1} - i\omega)}{(\tau_{\text{dis}}^{-1} - i\omega) (\delta^{-1} \tau_{22}^{-1} + \tau_{\text{dis}}^{-1} - i\omega) (\tau_{11}^{-1} + \tau_{\text{dis}}^{-1} - i\omega) + \omega_B^2 [\delta_3 \tau_{22}^{-1} + \delta_4 (\tau_{\text{dis}}^{-1} - i\omega)]}, \quad (31)$$

where

$$\delta_3 = \frac{\delta_1}{\delta} - \delta_1^2 - 2 \frac{\delta_2}{\delta} \ln 2 \approx 0.88, \quad \delta_4 = \delta_1 - 2\delta_2 \ln 2 \approx 1.45.$$

At $\mathbf{B} = 0$, the expression (31) reproduces Eq. (24) as it should. At $\omega = 0$, I recover the positive, parabolic

while the Hall part is given by

$$\frac{\pi \omega_B}{2T \ln 2} \begin{pmatrix} 0 & \delta_1 & -\delta_2 \\ 1 & 0 & 0 \\ 2 \ln 2 & 0 & 0 \end{pmatrix} \mathbf{e}_B \times \begin{pmatrix} \delta \mathbf{j} \\ \delta \mathbf{j}_I \\ \delta \mathbf{j}_E/T \end{pmatrix},$$

where

$$\delta_1 = \frac{1}{\delta} - \frac{2\pi^2 \ln 2}{27\zeta(3)\delta} \approx 2.08, \quad \delta_2 = \frac{\pi^2 - 12 \ln^2 2}{27\zeta(3)\delta} \approx 0.45.$$

As a result, the three equations for macroscopic currents simplify admitting a simple analytical solution. This solution is analogous to the solution of the stationary equations leading to the zero-frequency conductivity, see Refs. 15,23.

The third such equation stems from Eq. (12) and allows one to express the correction to the energy current, $\delta \mathbf{j}_E$, in terms of the correction to the electric current, $\delta \mathbf{j}$,

$$\delta \mathbf{j}_E = -2(\ln 2) \frac{\omega_B T}{\tau_{\text{dis}}^{-1} - i\omega} \mathbf{e}_B \times \delta \mathbf{j}. \quad (30a)$$

The second equation determines the correction to the imbalance current

$$\delta \mathbf{j}_I = -\frac{\omega_B}{\tau_{\text{dis}}^{-1} - i\omega} \left[1 - \frac{\delta_1 \tau_{22}^{-1}}{\delta^{-1} \tau_{22}^{-1} + \tau_{\text{dis}}^{-1} - i\omega} \right] \mathbf{e}_B \times \delta \mathbf{j}. \quad (30b)$$

The first equation determines the electrical current

$$e\mathbf{E} = \frac{\pi}{2T \ln 2} (\tau_{11}^{-1} + \tau_{\text{dis}}^{-1} - i\omega) \delta \mathbf{j} + \frac{\pi \omega_B}{2T \ln 2} (\delta_1 \mathbf{e}_B \times \delta \mathbf{j}_I - \delta_2 \mathbf{e}_B \times \delta \mathbf{j}_E/T). \quad (30c)$$

Both of the corrections (30a) and (30b) are orthogonal to the electric current, hence $\delta \mathbf{j} \parallel \mathbf{E}$. This means that no orthogonal component of the current is generated, in other words, there is no classical Hall effect in graphene at charge neutrality, as expected. Substituting the relations (30a) and (30b) into Eq. (30c), I find

magnetoresistance previously found in Refs. 15,23,31.

Let me now estimate the relative value of various parameters in Eq. (31) using the data of Ref. 1. Measurements at charge neutrality yield the following value of the coupling constant, $\alpha_g = 0.23$. Using Eqs. (D2), this lead to the following estimates of the scattering rates at

a typical temperature 267 K

$$\tau_{11}^{-1} \approx 7.35 \text{ THz}, \quad \tau_{22}^{-1} \approx 4.17 \text{ THz}.$$

The disorder scattering rate at 267 K was estimated as

$$\tau_{\text{dis}}^{-1} \approx 0.8 \text{ THz}.$$

Finally, evaluating Eq. (10d) at a reference magnetic field, $B = 1 \text{ T}$, the frequency ω_B can be estimated as

$$\omega_B = \frac{|e|v_g^2 B}{2cT \ln 2} \approx 27.9 \text{ THz} \frac{B}{1 \text{ T}} \frac{300 \text{ K}}{T},$$

such that at 267 K and 0.1 T one finds $\omega_B \approx 3.13 \text{ THz}$. For comparison, $267 \text{ K} \rightarrow 34.96 \text{ THz}$, so the hydrodynamic picture is fully justified.

At higher frequencies and magnetic fields the hydrodynamic picture breaks down³¹ in the sense that the local equilibrium (underlying the traditional derivation of the hydrodynamic equations^{10,14,15,18}) cannot be formed. At the same time, the kinetic (Boltzmann) equation has a much wider range of applicability. Within linear response, the kinetic equation can be integrated to obtain the macroscopic equations for quasiparticle currents^{23,40} without referring to local equilibrium. Remarkably, these linear response equations coincide with the macroscopic current equations (10), (11a), and (12), see Ref. 15 for more details. On one hand, this means that the results for linear response quantities, e.g. the electrical conductivity, obtained within the hydrodynamic theory coincide with the results of the linear response theory. On the other hand, the result (31) which has not been worked out within the linear response theory has a wider regime of applicability than the concept of local equilibrium. Extending the range of frequencies and magnetic fields in Eq. (31) one arrives at the resonance-like picture illustrated in Fig. 4. Note that at these frequencies one typically assumes the system to be in the collisionless regime^{21,24–29}, where the optical conductivity is given by the universal value (up to weak interaction corrections)

$$\sigma_U(\omega) = \frac{\pi e^2}{2h} [1 + \mathcal{C}_\sigma \alpha_g(\omega)], \quad (32a)$$

where the renormalized coupling constant $\alpha_g(\omega)$ and the numerical coefficient are given by

$$\alpha_g(\omega) = \frac{\alpha_g}{1 + \frac{\alpha_g}{4} \ln \frac{\mathcal{D}}{\omega}}, \quad \mathcal{C}_\sigma \approx 0.01. \quad (32b)$$

Physically, the universal value (32) is due to interband transitions and is hence beyond the semiclassical Boltzmann equation discussed in this paper. One typically assumes that the solutions to the Boltzmann equation yield the conductivity decaying with frequency, such that in the high-frequency regime Eq. (32) dominates. In the hydrodynamic regime this is illustrated in Fig. 3, where the universal value (32) is shown by the horizontal red line. Extending the kinetic theory beyond the hydrodynamic regime leads to the cyclotron resonance at high frequencies where the solution to the Boltzmann equation dominates over Eq. (32), see Fig. 4.

B. Magnetoconductivity in the degenerate regime

In the degenerate or Fermi-liquid regime only one band contributes to electronic transport and hence $\mathbf{j} = \mathbf{j}_I$ with exponential accuracy (see above). At the same time, away from charge neutrality the dissipative corrections (14) depend on the hydrodynamic velocity \mathbf{u} and hence the “hydrodynamic” and “kinetic” contributions to conductivity become entangled. In this case, it seems more transparent to consider the macroscopic equations for the electrical and energy currents explicitly. As shown in Ref. 15, these equations are exactly the same as the macroscopic linear response equations considered in Ref. 23. Similar equations have been derived in Ref. 40.

The equation for the energy current is just the Navier-Stokes equation (3c). For a homogeneous flow the gradient terms and the time derivative of pressure vanish, see the above derivation of Eq. (16c), such that the equation takes the form

$$\mathbf{j}_E (\tau_{\text{dis}}^{-1} - i\omega) = v_g^2 e n \mathbf{E} + v_g^2 \frac{e}{c} \mathbf{j} \times \mathbf{B}. \quad (33a)$$

The equation for the electric current is given by Eq. (10). For a homogeneous flow this equation takes the form

$$\mathbf{j} (\tau_{\text{dis}}^{-1} - i\omega) = \frac{1}{2} v_g^2 \frac{\partial n}{\partial \mu} e \mathbf{E} + \omega_B \mathcal{K} \times e_B + \mathcal{I}_1^{ee}. \quad (33b)$$

To the leading order²³, $\mathbf{j}_E \approx \mu \mathbf{j}$, $\mathcal{K} \approx \mathbf{j}$, and $\mathcal{I}_1^{ee} \rightarrow 0$. In this case, the two equations (33) are identical yielding the standard Drude-like results⁴⁷

$$\sigma_{xx} = \frac{e^2 \mu \tau_{\text{dis}}}{\pi} \frac{1 - i\omega \tau_{\text{dis}}}{(1 - i\omega \tau_{\text{dis}})^2 + \omega_B^2 \tau_{\text{dis}}^2}, \quad (34a)$$

$$\sigma_{xy} = -\frac{e^2 \mu \tau_{\text{dis}}}{\pi} \frac{\omega_B \tau_{\text{dis}}}{(1 - i\omega \tau_{\text{dis}})^2 + \omega_B^2 \tau_{\text{dis}}^2}. \quad (34b)$$

Here the electric field is taken to be directed along the x -axis, the magnetic field – along the z -axis. Note that the electric field is assumed to be oscillating, $E \sim \exp(-i\omega t)$, and the magnetic field is assumed to be static. For $\omega = 0$, I recover the standard magnetoconductivity^{23,47}.

At $\mathbf{B} = 0$ the results (34) yield the Drude conductivity given by Eq. (19) where one has to set $x \rightarrow \infty$. The leading correction to the Drude result is given by Eq. (27) where both the correction in Eq. (19) and the kinetic contribution (26b) are taken into account.

The origin of these corrections is in the differences between the two equations (33). Indeed, setting $\mathbf{B} = 0$ and subtracting Eq. (33a) from Eq. (33b), one finds

$$\begin{aligned} \left(\mathbf{j} - \frac{\mathbf{j}_E}{\mu} \right) (\tau_{\text{dis}}^{-1} - i\omega) &= v_g^2 \left(\frac{1}{2} \frac{\partial n}{\partial \mu} - n \right) e \mathbf{E} + \mathcal{I}_1^{ee} \\ &= -\frac{\pi^2}{3x^2} \frac{\mu}{\pi} e \mathbf{E} + \mathcal{I}_1^{ee}, \end{aligned}$$

where I used the equilibrium carrier density and compressibility in the limit $x \rightarrow \infty$, see Appendix A, keeping only the leading power law term.

In the same limit, the collision integral \mathcal{I}_1^{ee} can be expressed in terms of the two currents as

$$\begin{aligned}\mathcal{I}_1^{ee} &= -\frac{1}{2}v_g T \frac{\partial n}{\partial \mu} \tau_{11}^{-1} \mathbf{h}^{(1)} \\ &= \frac{3x^2}{\pi^2} \frac{\tau_{11}^{-1}}{1 - \frac{\pi^2}{3x^2}} \left[\left(1 + \frac{\pi^2}{x^2}\right) \mathbf{j} - \left(1 + \frac{\pi^2}{3x^2}\right) \frac{\mathbf{j}_E}{\mu} \right].\end{aligned}$$

Note that although Eq. (9b) relates the function $\mathbf{h}^{(1)}$ to the dissipative corrections $\delta \mathbf{j}$ and $\delta \mathbf{j}_E$, the hydrodynamic part of the macroscopic currents does not contribute to the collision integral as can be seen from the above expression by direct substitution.

Finally, the difference in the Lorentz terms in Eqs. (33) can be found by evaluating the quantity \mathcal{K} to the sub-leading order

$$\mathcal{K} = \frac{1}{1 - \frac{\pi^2}{3x^2}} \left(2\mathbf{j} - \frac{\mathbf{j}_E}{\mu} \right).$$

Using the above expressions, solving Eqs. (33) is a straightforward although tedious task. The result can be expressed as

$$\sigma_{xx} = \frac{e^2 \mu \tau_{\text{dis}}}{\pi} \frac{(1 - i\omega \tau_{\text{dis}}) \left[S_0 + \frac{\omega_B^2 \tau_{\text{dis}}^2 S_1 S_2}{(1 - i\omega \tau_{\text{dis}})^2} \right]}{(1 - i\omega \tau_{\text{dis}})^2 + \omega_B^2 \tau_{\text{dis}}^2 S_1^2}, \quad (35a)$$

$$\sigma_{xy} = -\frac{e^2 \mu \tau_{\text{dis}}}{\pi} \frac{\omega_B \tau_{\text{dis}} (S_0 S_1 - S_2)}{(1 - i\omega \tau_{\text{dis}})^2 + \omega_B^2 \tau_{\text{dis}}^2 S_1^2}, \quad (35b)$$

where

$$S_0 = 1 - \frac{\tau_{11}^{-1} [(3x^2/\pi^2)\tau_{11}^{-1} + \tau_{\text{dis}}^{-1} - i\omega]}{[(3x^2/\pi^2)\tau_{11}^{-1} + \tau_{\text{dis}}^{-1} - i\omega]^2 + \omega_B^2},$$

$$S_1 = 1 - \frac{3\tau_{11}^{-1} [(3x^2/\pi^2)\tau_{11}^{-1} + \tau_{\text{dis}}^{-1} - i\omega]}{[(3x^2/\pi^2)\tau_{11}^{-1} + \tau_{\text{dis}}^{-1} - i\omega]^2 + \omega_B^2},$$

$$S_2 = \frac{\pi^2}{3x^2} \frac{(\tau_{\text{dis}}^{-1} - i\omega)^2}{[(3x^2/\pi^2)\tau_{11}^{-1} + \tau_{\text{dis}}^{-1} - i\omega]^2 + \omega_B^2}.$$

In the limit $x \rightarrow \infty$, one finds $S_0 = S_1 = 1$, $S_2 = 0$ and one recovers Eqs. (33). For $\mathbf{B} = 0$, the result (35a) coincides with Eq. (27).

V. DISCUSSION

In this paper I have considered optical conductivity in graphene in the hydrodynamic regime. Within the hydrodynamic approach, the electric current is split into the hydrodynamic and kinetic contributions, see Eq. (3h), with the latter representing the dissipative correction. Unlike the traditional hydrodynamics¹³ in systems with

exact momentum conservation, the hydrodynamic equations in graphene include weak impurity scattering. As a result, both contributions to the electric current decay yielding Eqs. (17) and (15b).

Exactly at the neutrality point, the hydrodynamic contribution to electric current [and hence the conductivity (17)] vanishes. In this case, the optical conductivity in graphene is given by Eq. (21) illustrated in Fig. 1. Assuming the disorder scattering time in Eq. (21) to be negligibly small, one recovers the result of Ref. 32. This result was recently used in Ref. 1 to establish the experimental value of the electron-electron scattering time and ultimately the coupling constant, α_g . In the experiment, one treats α_g as a fitting parameter using the expression $\tau_{11}^{-1} = C\alpha_g^2 T$, with the numerical coefficient C calculated in Refs. 14,15,32,37,38 assuming the unscreened Coulomb interaction. Such approach can be justified³² by $1/N$ expansion suggesting that all interaction effects including screening and renormalization are confined to establishing the value of the effective coupling constant but do not significantly alter the momentum dependence of the matrix elements of the Coulomb interaction³⁸ (in the typical momentum range contributing to the collision integral).

At high enough doping levels, the electronic system in graphene is degenerate and most results resemble their counterparts in the usual Fermi liquid. In particular, the optical conductivity is given by Eq. (19). This expression is independent of the electron-electron scattering rate, which could be interpreted as “restoration” of Galilean invariance in the Fermi liquid regime. This result is fully “hydrodynamic” whereas the kinetic contribution to conductivity vanishes in this limit.

At intermediate carrier densities, the electrical conductivity is determined by the interplay of the above two mechanisms. While the hydrodynamic contribution keeps the simple form (17), the general expression for the kinetic contribution, Eq. (14), is extremely cumbersome. It is therefore tempting to use the interpolation formula, Eq. (1), instead. As evidenced by the leading corrections in both limits, Eqs. (27) and (28), the “exact” result (15b) differs from Eq. (1). However, the resulting optical conductivity is still roughly Lorentzian and hence could be fit by Eq. (1) using the two scattering rates as fitting parameters. Such approach was adopted in Ref. 1 (even the electronic temperature was obtained from the fit).

External magnetic field further complicates the theory by entangling the two contributions to the electric current. While not affecting the leading-order behavior in the degenerate regime, Eq. (34), the leading correction to the Drude behavior, Eq. (35), is dominated by the coupling between the two modes. At charge neutrality, the homogeneous electric current is still unaffected by the coupling to the hydrodynamic modes, but this is expected to change in finite size samples where the flow becomes inhomogeneous. Previously, this physics was used to explain giant magnetodrag in graphene⁴⁸ and to predict linear magnetoresistance in classically strong magnetic fields^{23,36,49}.

Finally, linear response transport in electronic systems can be described within the kinetic theory in wider parameter range as compared to the applicability region of hydrodynamics. The latter assumes that strong electron-electron interaction establishes local equilibrium^{14,15} describing the ideal hydrodynamic flow. In contrast, the linear response theory²³ assumes that in the absence of external fields the system is in the global equilibrium state described by the Fermi-Dirac distribution function and characterized by vanishing currents. Here the currents appear only as a response to the external electric field. Remarkably, linearizing the hydrodynamic equations in graphene (in order to find the linear response coefficients, such as electrical conductivity) yields exactly the same macroscopic equations [e.g., Eqs. (33)] as in the linear response theory rendering these equations more general than the concept of local equilibrium. Consequently, the results for optical conductivity obtained in this paper are valid in a wider frequency range than expected from the purely hydrodynamic perspective. This conclusion is most pronounced for the cyclotron resonance in moderately strong magnetic fields, see Fig. 4, where the kinetic contribution to the magnetoconductivity at relatively large frequencies dominates the universal free electron conductivity (32) describing the high-frequency collisionless regime that is not included in the semiclassical Boltzmann approach^{24,26}. A discussion of the quantum kinetic equation²⁴ including the interband transitions responsible for Eq. (32) is beyond the scope of this paper and will be reported elsewhere.

Acknowledgments

I thank A.D. Mirlin, J. Schmalian, M. Schütt, and especially I.V. Gornyi for numerous fruitful discussions. This work was supported by the German Research Foundation DFG within the FLAG-ERA Joint Transnational Call (Project GRANSPORE), by the European Commission under the EU Horizon 2020 MSCA-RISE-2019 program (Project 873028 HYDROTRONICS), and the MEPHI Academic Excellence Project, Contract No. 02.a03.21.0005.

Appendix A: Local equilibrium quantities

Under the assumption of local equilibrium, the macroscopic quantities appearing in the hydrodynamic theory can be computed explicitly¹⁵. The quasiparticle densities and the energy density have the following form

$$n = n_+ - n_- = \frac{T^2}{v_g^2} \frac{g_2(\mu_+/T) - g_2(-\mu_-/T)}{(1 - u^2/v_g^2)^{3/2}}, \quad (\text{A1a})$$

$$n_I = n_{+,0} + n_- = \frac{T^2}{v_g^2} \frac{g_2(\mu_+/T) + g_2(-\mu_-/T)}{(1 - u^2/v_g^2)^{3/2}}, \quad (\text{A1b})$$

$$n_E = 2 \frac{T^3}{v_g^2} \frac{1 + u^2/(2v_g^2)}{(1 - u^2/v_g^2)^{5/2}} \left[g_3\left(\frac{\mu_+}{T}\right) + g_3\left(-\frac{\mu_-}{T}\right) \right], \quad (\text{A1c})$$

where

$$g_2\left(\frac{\mu}{T}\right) = -\frac{N}{2\pi} \text{Li}_2\left(-e^{\mu/T}\right), \quad (\text{A2})$$

$$g_3\left(\frac{\mu}{T}\right) = -\frac{N}{2\pi} \text{Li}_3\left(-e^{\mu/T}\right), \quad (\text{A3})$$

with Li_n being the polylogarithm. It is convenient to express the densities (A1) in the dimensionless form

$$n = \frac{NT^2}{2\pi v_g^2} \tilde{n}, \quad n_I = \frac{NT^2}{2\pi v_g^2} \tilde{n}_I, \quad n_E = \frac{NT^3}{\pi v_g^2} \tilde{n}_E. \quad (\text{A4})$$

In the simplest case considered in this paper, $\mu_{\pm} = \mu$, the dimensionless imbalance density simplifies to

$$\tilde{n}_I = \frac{x^2}{2} + \frac{\pi^2}{6}, \quad x = \frac{\mu}{T}. \quad (\text{A5})$$

Similarly, the compressibilities (for $\mu_{\pm} = \mu$) are given by

$$\frac{\partial n}{\partial \mu} = \frac{NT}{2\pi v_g^2}, \quad \frac{\partial n_I}{\partial \mu} = \frac{N\mu}{2\pi v_g^2}, \quad \mathcal{T} = 2T \ln \left[2 \cosh \frac{x}{2} \right]. \quad (\text{A6})$$

The two thermodynamic quantities in the hydrodynamic theory, the pressure and enthalpy are given by

$$P = n_E \frac{1 - u^2/v_g^2}{2 + u^2/v_g^2}, \quad (\text{A7a})$$

$$W = n_E + P = \frac{3n_E}{2 + u^2/v_g^2}. \quad (\text{A7b})$$

They can be used to determine the stress-energy tensor

$$\Pi_E^{\alpha\beta} = P\delta_{\alpha\beta} + v_g^{-2} W u_{\alpha} u_{\beta}, \quad (\text{A8})$$

and the energy current (proportional to the momentum density $\mathbf{n}_{\mathbf{k}}$)

$$\mathbf{j}_E = v_g^2 \mathbf{n}_{\mathbf{k}} = W \mathbf{u}. \quad (\text{A9})$$

This relation is the key feature of the hydrodynamic description of the electronic system in graphene showing that it is the energy and not electric current that is described by the hydrodynamic flow. The quasiparticle currents are determined by the corresponding densities

$$\mathbf{j} = n\mathbf{u}, \quad \mathbf{j}_I = n_I \mathbf{u}. \quad (\text{A10})$$

Unlike the energy current, the quasiparticle currents are not conserved in electron-electron collisions and hence acquire the dissipative corrections (3h). Furthermore, the energy current can be relaxed by disorder scattering and hence acquires a dissipative correction of its own.

Appendix B: Collision integral

The integrated collision integrals (13d) are expressed in terms of the following scattering rates¹⁵

$$\frac{1}{\tau_{11}} = \pi^2 \alpha_g^2 NT \left[\frac{NT}{v_g^2 \partial n_0 / \partial \mu} \right] \int \frac{d^2 Q}{(2\pi)^2} \frac{dW}{2\pi} \frac{|\tilde{U}|^2}{\sinh^2 W} (Y_{00} Y_{11} - Y_{01}^2), \quad (\text{B1a})$$

$$\frac{1}{\tau_{12}} = \pi^2 \alpha_g^2 NT \left[\frac{NT}{v_g^2 \partial n_0 / \partial \mu} \right] \int \frac{d^2 Q}{(2\pi)^2} \frac{dW}{2\pi} \frac{|\tilde{U}|^2}{\sinh^2 W} (Y_{00} Y_{12} - Y_{02} Y_{01}), \quad (\text{B1b})$$

$$\frac{1}{\tau_{22}} = \pi^2 \alpha_g^2 NT \left[\frac{NT}{v_g^2 \partial n_0 / \partial \mu} \right] \int \frac{d^2 Q}{(2\pi)^2} \frac{dW}{2\pi} \frac{|\tilde{U}|^2}{\sinh^2 W} (Y_{00} Y_{22} - Y_{02}^2), \quad (\text{B1c})$$

with

$$Y_{00}(\omega, \mathbf{q}) = \frac{1}{4\pi} \left[\frac{\theta(|\Omega| \leq 1)}{\sqrt{1-\Omega^2}} \mathcal{Z}_0^>[I_1] + \frac{\theta(|\Omega| \geq 1)}{\sqrt{\Omega^2-1}} \mathcal{Z}_0^<[I_1] \right], \quad (\text{B2a})$$

$$Y_{01}(\omega, \mathbf{q}) = -\frac{1}{2\pi} \left[\theta(|\Omega| \leq 1) \sqrt{1-\Omega^2} \mathcal{Z}_2^>[I] + \theta(|\Omega| \geq 1) \sqrt{\Omega^2-1} \mathcal{Z}_2^<[I] \right], \quad (\text{B2b})$$

$$Y_{02}(\omega, \mathbf{q}) = \frac{1}{2\pi} \left[\theta(|\Omega| \leq 1) \sqrt{1-\Omega^2} \mathcal{Z}_3^>[I_1] + \theta(|\Omega| \geq 1) \frac{|\Omega|}{\sqrt{\Omega^2-1}} \mathcal{Z}_3^<[I_1] \right], \quad (\text{B2c})$$

$$Y_{11}(\omega, \mathbf{q}) = \frac{1}{\pi} \left[\theta(|\Omega| \leq 1) \sqrt{1-\Omega^2} \mathcal{Z}_1^>[I_1] + \theta(|\Omega| \geq 1) \sqrt{\Omega^2-1} \mathcal{Z}_1^<[I_1] \right], \quad (\text{B2d})$$

$$Y_{12}(\omega, \mathbf{q}) = -\frac{1}{\pi} \theta(|\Omega| \leq 1) \sqrt{1-\Omega^2} \mathcal{Z}_1^>[I], \quad (\text{B2e})$$

$$Y_{22}(\omega, \mathbf{q}) = \frac{1}{\pi} \left[\theta(|\Omega| \leq 1) \sqrt{1-\Omega^2} \mathcal{Z}_1^>[I_1] + \frac{\theta(|\Omega| \geq 1)}{\sqrt{\Omega^2-1}} \mathcal{Z}_3^<[I_1] \right], \quad (\text{B2f})$$

where

$$\mathcal{Z}_0^>[I] = \int_1^\infty dz \sqrt{z^2-1} I(z), \quad \mathcal{Z}_0^<[I] = \int_0^1 dz \sqrt{1-z^2} I(z), \quad (\text{B3a})$$

$$\mathcal{Z}_1^>[I] = \int_1^\infty dz \frac{\sqrt{z^2-1}}{z^2-\Omega^2} I(z), \quad \mathcal{Z}_1^<[I] = \int_0^1 dz \frac{\sqrt{1-z^2}}{\Omega^2-z^2} I(z), \quad (\text{B3b})$$

$$\mathcal{Z}_2^>[I] = \int_1^\infty dz \frac{z\sqrt{z^2-1}}{z^2-\Omega^2} I(z), \quad \mathcal{Z}_2^<[I] = \int_0^1 dz \frac{z\sqrt{1-z^2}}{\Omega^2-z^2} I(z), \quad (\text{B3c})$$

$$\mathcal{Z}_3^>[I] = \int_1^\infty dz \frac{(z^2-1)^{3/2}}{z^2-\Omega^2} I(z), \quad \mathcal{Z}_3^<[I] = \int_0^1 dz \frac{(1-z^2)^{3/2}}{\Omega^2-z^2} I(z). \quad (\text{B3d})$$

The functions I and I_1 are given by

$$I_1(z) = \tanh \frac{zQ+W+x}{2} + \tanh \frac{zQ+W-x}{2} - \tanh \frac{zQ-W+x}{2} - \tanh \frac{zQ-W-x}{2}, \quad (\text{B4a})$$

$$I(z) = \tanh \frac{zQ+W+x}{2} - \tanh \frac{zQ+W-x}{2} - \tanh \frac{zQ-W+x}{2} + \tanh \frac{zQ-W-x}{2}. \quad (\text{B4b})$$

The scattering rates (B1) can be expressed in terms of dimensionless integrals as

$$\tau_{ij}^{-1} = \frac{\alpha_g^2 NT}{16\pi^2} \left[\frac{NT}{v_g^2 \partial n / \partial \mu} \right] t_{ij}^{-1}, \quad (\text{B5})$$

which form the elements of the matrix $\widehat{\boldsymbol{\tau}}$, see Eqs. (13).

In the above integrals the frequency and momentum are expressed in terms of the dimensionless variables

$$\boldsymbol{Q} = \frac{v_g \boldsymbol{q}}{2T}, \quad W = \frac{\omega}{2T}. \quad (\text{B6})$$

Finally, the Coulomb interaction has the form

$$U(\omega, \boldsymbol{q}) = \frac{2\pi e^2}{q} \tilde{U} = \frac{2\pi \alpha_g v_g}{q} \tilde{U}, \quad \alpha_g = \frac{e^2}{v_g \varepsilon}, \quad (\text{B7})$$

where ε is the dielectric constant of the environment and the dimensionless factor \tilde{U} accounts for screening.

Appendix C: Collision integral in the degenerate regime

Here I evaluate the electron-electron scattering rates (B1) in the degenerate (or Fermi-liquid) regime.

Consider first the functions (B4). In the degenerate regime, $\mu \gg T$, but the frequency ω is of order T , i.e., $W \sim 1$. As a result, $W \ll x$, and one can expand the functions (B4) in W . The expansion is simplified by the following observation. For $x \gg 1$, the difference between two hyperbolic tangents is sharply peaked at $zQ \sim x$. For positive z one finds

$$I_1(z; x \gg 1) \approx -I(z; x \gg 1) \approx I_P(z; x \gg 1), \quad (\text{C1a})$$

$$I_P(z) = \tanh \frac{zQ + W - x}{2} - \tanh \frac{zQ - W - x}{2}. \quad (\text{C1b})$$

The relaxation rates (B1) comprise two integrals each, one over large and another over small values of the integration variable z , $z \geq 1$ and $0 \geq z \geq -1$, respectively. For small z , the peak at $zQ \sim x$ translates into very large values of the momentum, $Q > x$. At the same time, typical values of the frequency are of order temperature, $W \sim 1$, meaning $W \ll x$ and hence $|\Omega| = |W|/Q \ll 1$. This conclusion has the following two consequences.

First, only the region $|\Omega| < 1$ contributes to the scattering rates (up to exponentially small corrections, see below), hence one only needs to evaluate the integrals (B3) over $z > 1$. Taking into account Eq. (C1), I find that all three relaxation rates (B1) coincide,

$$\tau_{11} = \tau_{12} = \tau_{22}, \quad (\text{C2})$$

such that the matrix of the relaxation rates is degenerate even in the 2×2 sector. This degeneracy is due to the fact that in this regime only one band contributes to any physical quantity.

Second, the calculation of the single remaining rate, τ_{11}^{-1} , can be simplified by expanding the function I_P in powers of W ,

$$I_P(z) \approx \frac{2W}{1 + \cosh(zQ - x)} + \frac{W^3}{3} \frac{\cosh(zQ - x) - 2}{[1 + \cosh(zQ - x)]^2}. \quad (\text{C3})$$

Noticing that the integrand in Eq. (B1a) is an even function of W and at the same time is independent of the direction of \boldsymbol{Q} , the integral can be simplified as

$$\tau_{11}^{-1} = \alpha_g^2 \frac{N}{4\pi} \frac{T^2}{\mu} \int_0^\infty \frac{dW}{\sinh^2 W} \int_W^\infty Q dQ |\tilde{U}|^2 \left[\mathcal{Z}_0^\> [I_P] \mathcal{Z}_1^\> [I_P] - (1 - \Omega^2) (\mathcal{Z}_2^\> [I_P])^2 \right]. \quad (\text{C4})$$

The function (C1) depends only on the combination of variables, $y = zQ - x$. Changing the integration variable to y , I find for the three functions $\mathcal{Z}_i^\>$ appearing in Eq. (C4)

$$\mathcal{Z}_0^\> [I_P] = \frac{1}{Q^2} \int_{Q-x}^\infty dy I_P(y, W) \sqrt{(x+y)^2 - Q^2} \approx \frac{1}{Q^2} \left[x J_0 \sqrt{1 - \frac{Q^2}{x^2}} + \frac{J_1}{\sqrt{1 - \frac{Q^2}{x^2}}} - \frac{J_2 Q^2}{2x^3 \left(1 - \frac{Q^2}{x^2}\right)^{3/2}} \right], \quad (\text{C5a})$$

$$\begin{aligned} \mathcal{Z}_1^\> [I_P] &= \int_{Q-x}^\infty dy I_P(y, W) \frac{\sqrt{(x+y)^2 - Q^2}}{(x+y)^2 - W^2} \approx \frac{J_0}{x} \frac{\sqrt{1 - \frac{Q^2}{x^2}}}{1 - \frac{W^2}{x^2}} - \frac{J_1}{x^2} \frac{1 + \frac{W^2}{x^2} - 2\frac{Q^2}{x^2}}{\sqrt{1 - \frac{Q^2}{x^2}} \left(1 - \frac{W^2}{x^2}\right)^2} \\ &\quad + \frac{J_2}{x^3} \frac{1 + 3\frac{W^2}{x^2} - \frac{Q^2}{2x^2} \left(3 + \frac{W^2}{x^2}\right)^2 + \frac{Q^4}{x^4} \left(3 + \frac{W^2}{x^2}\right)}{\left(1 - \frac{Q^2}{x^2}\right)^{3/2} \left(1 - \frac{W^2}{x^2}\right)^3}, \end{aligned} \quad (\text{C5b})$$

$$\mathcal{Z}_2^>[I_P] = \frac{1}{Q} \int_{Q-x}^{\infty} dy I_P(y, W) \frac{(x+y)\sqrt{(x+y)^2 - Q^2}}{(x+y)^2 - W^2} \approx J_0 \frac{\sqrt{1 - \frac{Q^2}{x^2}}}{1 - \frac{W^2}{x^2}} + \frac{J_1}{x} \frac{\frac{Q^2}{x^2} \left(1 + \frac{W^2}{x^2}\right) - 2\frac{W^2}{x^2}}{\sqrt{1 - \frac{Q^2}{x^2}} \left(1 - \frac{W^2}{x^2}\right)^2} \quad (\text{C5c})$$

$$- \frac{J_2}{x^2} \frac{\frac{Q^2}{2x^2} \left(1 + 3\frac{W^2}{x^2}\right) \left(3 + \frac{W^2}{x^2}\right) - \frac{W^2}{x^2} \left(3 + \frac{W^2}{x^2}\right) - \frac{Q^4}{x^4} \left(1 + 3\frac{W^2}{x^2}\right)}{\left(1 - \frac{Q^2}{x^2}\right)^{3/2} \left(1 - \frac{W^2}{x^2}\right)^3},$$

where

$$J_n = \int_{Q-x}^{\infty} dy I_P(y, W) y^n, \quad (\text{C6})$$

and the expansion of the algebraic functions in Eqs. (C5) is justified by the fact that the function $I_P(y)$ has a form of a sharp peak centered at $y = 0$ [and in fact exponentially decaying beyond $y \sim 1$ as can be seen from the expansion (C3)], while $x \gg 1$.

Assuming $W \ll x$ in the degenerate limit, I now disregard the factors W^2/x^2 in the algebraic functions in Eqs. (C5) and form the integrand in Eq. (C4) as (alternatively one can integrate the algebraic functions over momentum while keeping the frequency finite and then compute the limit $x \rightarrow \infty$; the results for both the leading and subleading terms are the same)

$$\mathcal{Z}_0^>[I_P] \mathcal{Z}_1^>[I_P] - (1 - \Omega^2) (\mathcal{Z}_2^>[I_P])^2 \approx \frac{1}{Q^2} \left(1 - \frac{Q^2}{x^2}\right) \left[J_0^2 \frac{W^2}{Q^2} + \frac{J_0 J_2 - J_1^2}{x^2} - \frac{J_0 J_2}{x^2} \frac{Q^2}{x^2} \frac{\frac{11}{2} - 4\frac{Q^2}{x^2}}{\left(1 - \frac{Q^2}{x^2}\right)^2} + \dots \right], \quad (\text{C7})$$

where the frequency in the first term comes from the factor $1 - \Omega^2$ in Eq. (C4), which cannot be neglected before one determines the order of magnitude of the typical values of Q in the integral in Eq. (C4).

Consider now the functions J_n . The integral for $n = 0$ yields [the exact result is followed by an approximation obtained by integrating Eq. (C3); the same approximation can be obtained by series expansion]

$$J_0 = 2 \left[W - \ln(e^{Q+W} + e^x) + \ln(e^Q + e^{x+W}) \right] \approx 2W \left(1 + \tanh \frac{x-Q}{2} \right) - \frac{4W^3}{3} \frac{\sinh^4 \frac{x-Q}{2}}{\sinh^3(x-Q)} \approx 4W\theta(Q < x), \quad (\text{C8a})$$

where the second equality can be directly obtained by using the first term in the expansion (C3).

The other functions J_n cannot be integrated in a closed form. One can either evaluate them approximately using the leading order expansion (C3) or compute them numerically. The approximate calculation yields

$$J_0^2 \approx 16W^2\theta(Q < x), \quad J_0 J_2 - J_1^2 \approx J_0 J_2 \approx \frac{16(\pi^2 + 1)}{3} W^2 \theta(Q + 2 < x). \quad (\text{C8b})$$

Substituting the first term in Eq. (C7) into Eq. (C4) I find

$$t_1 = \alpha_g^2 \frac{N}{4\pi} \frac{T^2}{\mu} \int_0^{\infty} \frac{dW}{\sinh^2 W} \int_W^{\infty} Q dQ |\tilde{U}|^2 \frac{W^2}{Q^4} \left(1 - \frac{Q^2}{x^2}\right) J_0^2 \approx \alpha_g^2 \frac{4N}{\pi} \frac{T^2}{\mu} \int_0^{\infty} \frac{dW W^4}{\sinh^2 W} \int_W^x \frac{dQ}{Q^3} \left(1 - \frac{Q^2}{x^2}\right) |\tilde{U}|^2.$$

For bare Coulomb interaction, $|\tilde{U}|^2 = 1$, I evaluate the integrals as

$$\int_0^{\infty} \frac{dW W^4}{\sinh^2 W} \int_W^x \frac{dQ}{Q^3} \left(1 - \frac{Q^2}{x^2}\right) = \frac{1}{2} \int_0^{\infty} \frac{dW W^4}{\sinh^2 W} \left(\frac{1}{W^2} - \frac{1}{x^2} - \frac{2}{x^2} \ln \frac{x}{W} \right) = \frac{\pi^2}{12} - \frac{\pi^4}{60x^2} \left(1 + 2 \ln \frac{\gamma\mu}{T}\right), \quad \gamma = 0.474.$$

For statically screened Coulomb, $|\tilde{U}|^2 = Q^2/(Q + \varkappa)^2$, where the Thomas-Fermi screening yields $\varkappa = N\alpha_g x$, I find

$$\int_W^x \frac{dQ}{Q} \frac{\left(1 - \frac{Q^2}{x^2}\right)}{(Q + \varkappa)^2} = \left[\frac{1}{\varkappa^2} - \frac{1}{x^2} \right] \left[\frac{W}{W + \varkappa} - \frac{x}{x + \varkappa} \right] + \left[\frac{1}{\varkappa^2} + \frac{1}{x^2} \right] \left[\ln \frac{x}{x + \varkappa} - \ln \frac{W}{W + \varkappa} \right] + \frac{1}{x^2} \ln \frac{W}{x},$$

which recovers the above result in the limit $\varkappa \rightarrow 0$. The limit $x \rightarrow \infty$ here is non-trivial since $\varkappa \propto x$ and one can discern three regimes: $\varkappa \ll 1$, $1 \ll \varkappa \ll x$, and $\varkappa \gg x$. In the first regime, the integral differs from the above result for $\varkappa = 0$ by small corrections. The last regime has only a formal interest, since in order to achieve this one has to consider large α_g contradicting the assumptions of the present approach. In the second regime, the above expression can be represented as a series expansion in x^{-1} . For not too small $\alpha_g \gtrsim 0.1$

$$\int_W^x \frac{dQ}{Q} \frac{\left(1 - \frac{Q^2}{x^2}\right)}{(Q + \varkappa)^2} = \frac{1}{N^2 \alpha_g^2 x^2} \left[\ln \frac{N \alpha_g}{W} - g(\alpha_g) \right] + \frac{W}{2N^2 \alpha_g^3 x^3} + \mathcal{O}(x^{-4}),$$

where

$$g(\alpha_g) = 1 - N \alpha_g + \ln(1 + N \alpha_g) + N^2 \alpha_g^2 \ln \frac{1 + N \alpha_g}{N \alpha_g}, \quad g(\alpha_g \gtrsim 0.25) \approx \ln(1 + N \alpha_g) + \frac{1}{2}.$$

Note that the subleading term in this expansion is essential since the leading term changes sign at not too large W , while the integral is explicitly positive. Integrating over the frequencies, I find

$$\int_0^\infty \frac{dW W^4}{\sinh^2 W} \int_W^x \frac{dQ}{Q} \frac{\left(1 - \frac{Q^2}{x^2}\right)}{(Q + \varkappa)^2} = \frac{\pi^4}{30 N^2 \alpha_g^2 x^2} [\ln(\gamma N \alpha_g) - g(\alpha_g)] + \frac{15\zeta(5)}{4 N^2 \alpha_g^3 x^3}.$$

Again, while formally subleading in the limit $x \rightarrow \infty$, the second term is important since for small α_g the first term is negative.

Consider now the contribution of the second term in Eq. (C7). Similarly to the above, I find

$$t_2 = \alpha_g^2 \frac{N}{4\pi} \frac{T^2}{\mu} \int_0^\infty \frac{dW}{\sinh^2 W} \int_W^\infty Q dQ \frac{1}{Q^2} \left(1 - \frac{Q^2}{x^2}\right) \frac{J_0 J_2 - J_1^2}{x^2} \approx \alpha_g^2 \frac{4N}{3\pi} (\pi^2 + 1) \frac{T^2}{\mu x^2} \int_0^\infty \frac{dW W^4}{\sinh^2 W} \int_W^{x^{-2}} \frac{dQ}{Q} \left(1 - \frac{Q^2}{x^2}\right),$$

which in the limit $x \rightarrow \infty$ is clearly subleading to t_1 .

As a result, the “scattering rate” τ_{11}^{-1} in the degenerate regime is given by

$$\tau_{11}^{-1} \approx \frac{\pi N}{3} \alpha_g^2 \frac{T^2}{\mu}. \quad (\text{C9a})$$

for the unscreened Coulomb interaction. Taking into account screening, the result in the most interesting regime, $1 \ll \varkappa < x$ is

$$\tau_{11}^{-1} \approx \frac{T^4}{\mu^3} \left[\frac{\pi}{30} [\ln(\gamma N \alpha_g) - g(\alpha_g)] + \frac{15\zeta(5)}{4\pi \alpha_g x} \right]. \quad (\text{C9b})$$

One should keep in mind, however, that the Thomas-Fermi screening is nothing but the static limit of the random phase approximation (RPA). The latter is by no means exact, especially for not so small coupling constants. Hence including the RPA screening, but neglecting vertex corrections might not yield the better approximation to the exact result than the bare Coulomb interaction. At the neutrality point this is supported by $1/N$ expansion^{32,38} where one can show that for the momentum range dominating the integration the leading-order results are given by the unscreened Coulomb (perhaps, with the renormalized coupling constant). While no such analysis has been reported in the degenerate regime, the above statement seems plausible on physical grounds and hence Eq. (C9b) should be treated with care.

Appendix D: Collision integral close to charge neutrality

At charge neutrality $I(x=0) = 0$ and hence $\tau_{12}^{-1} = 0$. In vicinity of charge neutrality the dependence on the chemical potential (or on the dimensionless variable $x = \mu/T$) comes from the compressibility in the dimensionfull prefactor in Eq. (B5) and the functions I and I_1 determining the dimensionless scattering rates t_{ij}^{-1} .

The prefactor in Eq. (B5) can be expressed as follows

$$\frac{\alpha_g^2 N T}{16\pi^2} \left[\frac{N T}{v_g^2 \partial n / \partial \mu} \right] \approx \frac{\alpha_g^2 T}{4\pi \ln 2} \left(1 - \frac{x^2}{8 \ln 2} \right).$$

Expanding both functions (B4) for $x \ll 1$, one finds

$$I_1 = I_1^{(0)} + x^2 I_1^{(2)} + \mathcal{O}(x^3), \quad (\text{D1a})$$

$$I_1^{(0)} = \frac{4 \sinh W}{\cosh W + \cosh zQ},$$

$$I_1^{(2)} = \frac{2 \sinh W (\cosh 2zQ - 2 \cosh W \cosh zQ - 3)}{(\cosh W + \cosh zQ)^3}$$

$$I = -xI^{(1)} + \mathcal{O}(x^3), \quad I^{(1)} = 4 \frac{\sinh zQ \sinh W}{(\cosh W + \cosh zQ)^2}. \quad (\text{D1b})$$

Substituting these expansions into Eqs. (B1), one can establish the leading terms in the expansion of the scattering rates

$$\frac{1}{\tau_{11}} = \frac{\alpha_g^2 T}{4\pi \ln 2} \left[\frac{1}{t_{11}^{(0)}} + x^2 \left(\frac{1}{t_{11}^{(2)}} - \frac{1}{8 \ln 2} \frac{1}{t_{11}^{(0)}} \right) + \mathcal{O}(x^3) \right], \quad (\text{D2a})$$

$$\frac{1}{\tau_{12}} = \frac{\alpha_g^2 T}{4\pi \ln 2} \frac{x}{t_{12}^{(1)}} + \mathcal{O}(x^3), \quad (\text{D2b})$$

$$\frac{1}{\tau_{22}} = \frac{\alpha_g^2 T}{4\pi \ln 2} \left[\frac{1}{t_{22}^{(0)}} + x^2 \left(\frac{1}{t_{22}^{(2)}} - \frac{1}{8 \ln 2} \frac{1}{t_{22}^{(0)}} \right) + \mathcal{O}(x^3) \right]. \quad (\text{D2c})$$

The quantities $t_{ij}^{(0,1,2)}$ in Eqs. (D2) are the expansion coefficients of the dimensionless integral in Eq. (B5) close to the Dirac point in the self-evident notation similar to that in Eqs. (D1). For unscreened Coulomb interaction these quantities are just numbers without any dependence on any physical parameter. If screening is taken into account, then these numbers depend on the screening length, i.e. on a fixed combination of the coupling constant and temperature.

For unscreened Coulomb interaction, one finds the following numerical values (neglecting the small³⁷ exchange contribution):

$$\left(t_{11}^{(0)}\right)^{-1} \approx 33.13, \quad \left(t_{11}^{(2)}\right)^{-1} \approx 3.38,$$

$$\left(t_{12}^{(1)}\right)^{-1} \approx 5.45, \quad \left(t_{22}^{(0)}\right)^{-1} \approx 18.02, \quad \left(t_{22}^{(2)}\right)^{-1} \approx 4.73.$$

Appendix E: Optical conductivity close to charge neutrality

Inverting the matrix \mathbf{S}_{xx} using the identity

$$[\mathbf{S}_{xx}(0) + \delta\mathbf{S}_{xx}]^{-1} \approx \mathbf{S}_{xx}^{-1}(0) - \mathbf{S}_{xx}^{-1}(0)\delta\mathbf{S}_{xx}\mathbf{S}_{xx}^{-1}(0),$$

and substituting the result into the general expression (15b) together with the expansions of the matrices $\widehat{\mathbf{m}}_{h(n)}$, one finds the leading contribution to Eq. (24) as

$$\begin{aligned} \widehat{\mathbf{m}}_h \mathbf{S}_{xx}^{-1} \widehat{\mathbf{m}}_n &\approx \widehat{\mathbf{m}}_h \mathbf{S}_{xx}^{-1}(0) \widehat{\mathbf{m}}_n + \\ &+ \widehat{\mathbf{m}}_h(0) \mathbf{S}_{xx}^{-1}(0) \delta\mathbf{S}_{xx} \mathbf{S}_{xx}^{-1}(0) \widehat{\mathbf{m}}_n(0) \\ &+ \delta\widehat{\mathbf{m}}_h \mathbf{S}_{xx}^{-1}(0) \delta\mathbf{S}_{xx} \mathbf{S}_{xx}^{-1}(0) \widehat{\mathbf{m}}_n(0) \\ &+ \widehat{\mathbf{m}}_h(0) \mathbf{S}_{xx}^{-1}(0) \delta\mathbf{S}_{xx} \mathbf{S}_{xx}^{-1}(0) \delta\widehat{\mathbf{m}}_n. \end{aligned}$$

The first line comprises the zeroth order result, Eq. (24), and the correction

$$\delta\sigma_1(\omega) = \frac{\gamma_{11} e^2 T x^2}{-i\omega + \tau_{\text{dis}}^{-1} + \tau_{11}^{-1}(0)} + \frac{\gamma_{12} e^2 T x^2}{-i\omega + \tau_{\text{dis}}^{-1} + \gamma_{13} \tau_{22}^{-1}(0)},$$

where the scattering rates are evaluated at the Dirac point, $x = 0$, and the numerical coefficients are

$$\gamma_{11} = \frac{2 \ln 2}{\pi} \frac{8 \ln 2}{27\zeta(3)} \approx 0.17 \times \frac{2 \ln 2}{\pi} \approx 0.075,$$

$$\gamma_{12} = \frac{3[4\pi^2 \ln 2 - 27\zeta(3)]^2}{162\pi\zeta(3) \ln 2 - \pi^5} \approx 0.66,$$

$$\gamma_{13} = \frac{162\pi\zeta(3) \ln 2}{162\pi\zeta(3) \ln 2 - \pi^5} \approx 3.59.$$

The second line yields

$$\delta\sigma_2(\omega) = \frac{e^2 T x^2}{2\pi^2} \frac{\frac{1}{t_{11}^{(2)}} - \frac{1}{8 \ln 2} \frac{1}{t_{11}^{(0)}}}{[-i\omega + \tau_{\text{dis}}^{-1} + \tau_{11}^{-1}(0)]^2},$$

where the numerator represents the leading correction to the scattering rate τ_{11}^{-1} , see Eq. (D2a). Finally, the last two lines give rise to two similar contributions

$$\begin{aligned} \delta\sigma_3(\omega) &= \frac{e^2 T x^2}{-i\omega + \tau_{\text{dis}}^{-1} + \tau_{11}^{-1}(0)} \frac{1}{-i\omega + \tau_{\text{dis}}^{-1} + \gamma_{13} \tau_{22}^{-1}(0)} \\ &\times \left[\gamma_{31} \tau_{22}^{-1}(0) + \gamma_{32} (-i\omega + \tau_{\text{dis}}^{-1}) - \gamma_{33} / \tau_{12}^{(1)} \right], \end{aligned}$$

$$\begin{aligned} \delta\sigma_4(\omega) &= \frac{e^2 T x^2}{-i\omega + \tau_{\text{dis}}^{-1} + \tau_{11}^{-1}(0)} \frac{1}{-i\omega + \tau_{\text{dis}}^{-1} + \gamma_{13} \tau_{22}^{-1}(0)} \\ &\times \left[\gamma_{41} (-i\omega + \tau_{\text{dis}}^{-1}) + \gamma_{42} / \tau_{12}^{(1)} \right], \end{aligned}$$

where

$$\gamma_{31} = \frac{288 \ln^3 2}{162\pi\zeta(3) \ln 2 - \pi^5} \approx 0.81,$$

$$\gamma_{32} = \frac{3(96 \ln^3 2 + 27\zeta(3) - 8\pi^2 \ln 2)}{162\pi\zeta(3) \ln 2 - \pi^5} \approx 0.246,$$

$$\gamma_{33} = \frac{3[8\pi^2 \ln 2 - 27\zeta(3)]}{162\pi\zeta(3) \ln 2 - \pi^5} \approx 0.57,$$

$$\gamma_{41} = \frac{3[4\pi^2 \ln 2 - 27\zeta(3)][8\pi^2 \ln 2 - 54\zeta(3)]}{2(162\pi\zeta(3) \ln 2 - \pi^5)} \approx 0.66,$$

$$\gamma_{42} = \frac{81\zeta(3)[4\pi^2 \ln 2 - 27\zeta(3)]}{2\pi(162\pi\zeta(3) \ln 2 - \pi^5)} \approx 0.67.$$

- ¹ P. Gallagher, C.-S. Yang, T. Lyu, F. Tian, R. Kou, H. Zhang, K. Watanabe, T. Taniguchi, and F. Wang, *Science* **364**, 158 (2019).
- ² D. A. Bandurin, I. Torre, R. Krishna Kumar, M. Ben Shalom, A. Tomadin, A. Principi, G. H. Auton, E. Khestanova, K. S. Novoselov, I. V. Grigorieva, et al., *Science* **351**, 1055 (2016).
- ³ J. Crossno, J. K. Shi, K. Wang, X. Liu, A. Harzheim, A. Lucas, S. Sachdev, P. Kim, T. Taniguchi, K. Watanabe, et al., *Science* **351**, 1058 (2016).
- ⁴ F. Ghahari, H.-Y. Xie, T. Taniguchi, K. Watanabe, M. S. Foster, and P. Kim, *Phys. Rev. Lett.* **116**, 136802 (2016).
- ⁵ R. Krishna Kumar, D. A. Bandurin, F. M. D. Pellegrino, Y. Cao, A. Principi, H. Guo, G. H. Auton, M. Ben Shalom, L. A. Ponomarenko, G. Falkovich, et al., *Nature Physics* **13**, 1182 (2017).
- ⁶ D. A. Bandurin, A. V. Shytov, L. S. Levitov, R. K. Kumar, A. I. Berdyugin, M. Ben Shalom, I. V. Grigorieva, A. K. Geim, and G. Falkovich, *Nature Communications* **9**, 4533 (2018).
- ⁷ L. Ella, A. Rozen, J. Birkbeck, M. Ben-Shalom, D. Perello, J. Zultak, T. Taniguchi, K. Watanabe, A. K. Geim, S. Ilani, et al., *Nature Nanotechnology* **14**, 480 (2019).
- ⁸ A. I. Berdyugin, S. G. Xu, F. M. D. Pellegrino, R. K. Kumar, A. Principi, I. Torre, M. B. Shalom, T. Taniguchi, K. Watanabe, I. V. Grigorieva, et al., *Science* **364**, 162 (2019).
- ⁹ B. N. Narozhny, I. V. Gornyi, A. D. Mirlin, and J. Schmalian, *Annalen der Physik* **529**, 1700043 (2017).
- ¹⁰ A. Lucas and K. C. Fong, *Journal of Physics: Condensed Matter* **30**, 053001 (2018).
- ¹¹ M. J. H. Ku, T. X. Zhou, Q. Li, Y. J. Shin, J. K. Shi, C. Burch, H. Zhang, F. Casola, T. Taniguchi, K. Watanabe, et al., *Imaging Viscous Flow of the Dirac Fluid in Graphene Using a Quantum Spin Magnetometer* (2019), arXiv:1905.10791.
- ¹² J. A. Sulpizio, L. Ella, A. Rozen, J. Birkbeck, D. J. Perello, D. Dutta, M. Ben-Shalom, T. Taniguchi, K. Watanabe, T. Holder, et al., *Visualizing Poiseuille flow of hydrodynamic electrons* (2019), arXiv:1905.11662.
- ¹³ L. D. Landau and E. M. Lifshitz, *Fluid Mechanics* (Pergamon Press, London, 1959).
- ¹⁴ U. Briskot, M. Schütt, I. V. Gornyi, M. Titov, B. N. Narozhny, and A. D. Mirlin, *Phys. Rev. B* **92**, 115426 (2015).
- ¹⁵ B. N. Narozhny (2019), arXiv:1905.09686.
- ¹⁶ B. N. Narozhny and M. Schütt, *Phys. Rev. B* **100**, 035125 (2019).
- ¹⁷ M. S. Foster and I. L. Aleiner, *Phys. Rev. B* **79**, 085415 (2009).
- ¹⁸ E. M. Lifshitz and L. P. Pitaevskii, *Physical Kinetics* (Pergamon Press, London, 1981).
- ¹⁹ B. Bradlyn, M. Goldstein, and N. Read, *Phys. Rev. B* **86**, 245309 (2012).
- ²⁰ A. Principi, G. Vignale, M. Carrega, and M. Polini, *Phys. Rev. B* **93**, 125410 (2016).
- ²¹ J. M. Link, D. E. Sheehy, B. N. Narozhny, and J. Schmalian, *Phys. Rev. B* **98**, 195103 (2018).
- ²² G. Giuliani and G. Vignale, *Quantum Theory of the Electron Liquid* (Cambridge University Press, 2005).
- ²³ B. N. Narozhny, I. V. Gornyi, M. Titov, M. Schütt, and A. D. Mirlin, *Phys. Rev. B* **91**, 035414 (2015).
- ²⁴ E. G. Mishchenko, *EPL (Europhysics Letters)* **83**, 17005 (2008).
- ²⁵ S. Teber and A. V. Kotikov, *EPL (Europhysics Letters)* **107**, 57001 (2014).
- ²⁶ D. E. Sheehy and J. Schmalian, *Phys. Rev. B* **80**, 193411 (2009).
- ²⁷ J. M. Link, P. P. Orth, D. E. Sheehy, and J. Schmalian, *Phys. Rev. B* **93**, 235447 (2016).
- ²⁸ R. R. Nair, P. Blake, A. N. Grigorenko, K. S. Novoselov, T. J. Booth, T. Stauber, N. M. R. Peres, and A. K. Geim, *Science* **320**, 1308 (2008).
- ²⁹ T. Stauber, N. M. R. Peres, and A. K. Geim, *Phys. Rev. B* **78**, 085432 (2008).
- ³⁰ S. A. Hartnoll, P. K. Kovtun, M. Müller, and S. Sachdev, *Phys. Rev. B* **76**, 144502 (2007).
- ³¹ M. Müller, L. Fritz, and S. Sachdev, *Phys. Rev. B* **78**, 115406 (2008).
- ³² L. Fritz, J. Schmalian, M. Müller, and S. Sachdev, *Phys. Rev. B* **78**, 085416 (2008).
- ³³ M. Müller and S. Sachdev, *Phys. Rev. B* **78**, 115419 (2008).
- ³⁴ Z. Sun, D. N. Basov, and M. M. Fogler, *Proceedings of the National Academy of Sciences* **115**, 3285 (2018).
- ³⁵ I. L. Aleiner and B. I. Shklovskii, *Phys. Rev. B* **49**, 13721 (1994).
- ³⁶ P. S. Alekseev, A. P. Dmitriev, I. V. Gornyi, V. Y. Kachorovskii, B. N. Narozhny, M. Schütt, and M. Titov, *Phys. Rev. Lett.* **114**, 156601 (2015).
- ³⁷ A. B. Kashuba, *Phys. Rev. B* **78**, 085415 (2008).
- ³⁸ M. Schütt, P. M. Ostrovsky, I. V. Gornyi, and A. D. Mirlin, *Phys. Rev. B* **83**, 155441 (2011).
- ³⁹ D. E. Sheehy and J. Schmalian, *Phys. Rev. Lett.* **99**, 226803 (2007).
- ⁴⁰ F. M. D. Pellegrino, I. Torre, and M. Polini, *Phys. Rev. B* **96**, 195401 (2017).
- ⁴¹ T. Holder, R. Queiroz, and A. Stern, *Phys. Rev. Lett.* **123**, 106801 (2019).
- ⁴² T. Holder, R. Queiroz, T. Scaffidi, N. Silberstein, A. Rozen, J. A. Sulpizio, L. Ella, S. Ilani, and A. Stern, *Ballistic and hydrodynamic magnetotransport in narrow channels* (2019), arXiv:1901.08546.
- ⁴³ P. S. Alekseev, *Phys. Rev. B* **98**, 165440 (2018).
- ⁴⁴ D. Svintsov, *Phys. Rev. B* **97**, 121405(R) (2018).
- ⁴⁵ A. A. Kozikov, A. K. Savchenko, B. N. Narozhny, and A. V. Shytov, *Phys. Rev. B* **82**, 075424 (2010).
- ⁴⁶ G. X. Ni, L. Wang, M. D. Goldflam, M. Wagner, Z. Fei, A. S. McLeod, M. K. Liu, F. Keilmann, B. Özyilmaz, A. H. Castro Neto, et al., *Nature Photonics* **10**, 244 (2016).
- ⁴⁷ M. P. Marder, *Condensed Matter Physics* (Wiley, 2010).
- ⁴⁸ M. Titov, R. V. Gorbachev, B. N. Narozhny, T. Tudorovskiy, M. Schütt, P. M. Ostrovsky, I. V. Gornyi, A. D. Mirlin, M. I. Katsnelson, K. S. Novoselov, et al., *Phys. Rev. Lett.* **111**, 166601 (2013).
- ⁴⁹ G. Y. Vasileva, D. Smirnov, Y. L. Ivanov, Y. B. Vasilyev, P. S. Alekseev, A. P. Dmitriev, I. V. Gornyi, V. Y. Kachorovskii, M. Titov, B. N. Narozhny, et al., *Phys. Rev. B* **93**, 195430 (2016).